THE DISKS OF T TAURI STARS WITH FLAT INFRARED SPECTRA

FRED C. ADAMS
University of California, Berkeley

CHARLES J. LADA
Steward Observatory, University of Arizona, Tucson

AND

FRANK H. SHU
University of California, Berkeley

ABSTRACT

We model the energy distributions of T Tauri stars with flat infrared spectra by assuming that they have spatially thin disks with unorthodox radial gradients of temperature. These sources differ from more common T Tauri stars in that the extreme shallowness of their spectral slope cannot be plausibly explained by conventional ideas (e.g., Keplerian accretion or reprocessing of starlight by a slightly flared disk). Minimum values for the radii of the disks can be obtained by considering models that are optically thick at all observed wavelengths. Maximum values for the disk masses can be obtained if measurements of the dust continuum emission are available at low frequencies, where the disks are likely to be optically thin. The latter estimates are sensitive to the assumed dust opacities, which are somewhat uncertain at submillimeter and millimeter wavelengths. Derived model parameters show that the disks associated with the flat-spectrum sources must contain intrinsic luminosity in addition to the energy intercepted and reprocessed from the central star; i.e., the disks must be *active*. Self-gravity may provide one possible source for this activity—the spectral limits and estimates of the disk masses derived for three systems (T Tau, DG Tau, and HL Tau) are close to the theoretical values that would make the self-gravity of the disks dynamically important.

Subject headings: infrared: spectra — spectrophotometry — stars: accretion — stars: pre–main-sequence

I. INTRODUCTION

The infrared excesses of T Tauri stars have posed a puzzle for astronomers since the discovery of the phenomenon over two decades ago. As first suggested by Mendoza (1966, 1968), thermal emission from circumstellar dust grains is probably responsible for the observed IR excesses (see also the discussion of Cohen and Kuhi [1979], hereafter CK, concerning the inadequacy of free-free emission); however, the geometry of the distribution of emitting material has remained controversial. Proposals have included grain formation in the outflows from young stars and other spherical dust shells (see, e.g., Rowan-Robinson and Harris 1982, Wolfire and Churchwell 1987, and the review by Cohen 1984) and accretion disks (Lynden-Bell and Pringle 1974). The arguments for and against these various possibilities are briefly summarized in Shu, Adams, and Lizano (1987). Recently, observations of T Tauri stars in the mid- and far-infrared (e.g., Rydgren, Strom, and Strom 1976, Lada and Wilking 1984, and Rucinski 1985) have demonstrated that the infrared excess typically persists out to wavelengths as long as 100 μm. Moreover, the vast majority of T Tauri stars are found to have infrared energy distributions whose shapes longward of 2 μm are remarkably similar and can be characterized by power laws (e.g., Rucinski 1985, Rydgren and Zak 1987, and Lada 1987). These observations place strong constraints on theories for the origin of the excess emission.

In an earlier paper in this journal (Adams, Lada, and Shu 1987, hereafter Paper I), we proposed an evolutionary sequence for understanding the spectral energy distributions of young stellar objects (YSOs), beginning with protostars and ending with pre–main-sequence stars. In Paper I, we classified the spectral energy distributions of young stellar objects according to the spectral index,

$$n \equiv \frac{d \log (\nu F_\nu)}{d \log \nu} = -\frac{d \log (\lambda F_\lambda)}{d \log \lambda}, \tag{1}$$

which is to be evaluated in the near- to mid-infrared portion of the spectrum (i.e., from $\lambda = 1$–10 μm or $\nu = 10^{14.5}$–$10^{13.5}$ Hz). In this scheme, protostars have negative spectral indices, T Tauri stars with infrared excesses have positive or nearly zero spectral indices, and main-sequence stars or pre–main-sequence stars without appreciable circumstellar material (e.g., the "naked" T Tauri stars; see Walter 1987) have $n \approx 3$. In Paper I (see also Rucinski 1985, Beall 1987, Bertout 1987, and Kenyon and Hartmann 1987), we showed that the broad-band spectral energy distributions of T Tauri stars with infrared excesses can be explained in terms of star/disk systems, with the disks grouped into two basic categories: (*a*) *passive* disks which have negligible intrinsic luminosity, but intercept and reradiate $\frac{1}{4}$ of the stellar luminosity, and (*b*) *active* disks which have some intrinsic energy source in addition to reprocessing of stellar photons. A passive disk has a temperature distribution of the approximate form

$$T_D \propto \varpi^{-3/4} \tag{2}$$

(see the Appendix to Adams and Shu 1986 and the Appendix to this paper); this distribution produces a spectral index $n = 4/3$, the same as a classical Keplerian accretion disk (Lynden-Bell and Pringle 1974). The interpretation of T Tauri stars with excess infrared emission as star/disk systems has

recently been strengthened by the observation of nearly Keplerian differential rotation (Hartmann and Kenyon 1987) in the optical and near-infrared spectra of FU Ori, a young stellar object whose spectral energy distribution can be explained by a disk that produces a spectral index of 4/3 (see Paper I, Hartmann and Kenyon 1985). However, to produce a flat (i.e., $n \approx 0$) spectrum requires a nonconventional temperature distribution,

$$T_D \propto \varpi^{-1/2} , \qquad (3)$$

as was pointed out in Paper I but not examined in any detail (see also Elmegreen 1982b).

The flat spectrum sources are particularly interesting because they are often the most extreme in terms of all characteristics usually associated with T Tauri stars—infrared excess, ultraviolet excess, variability, emission lines, etc. (see Cohen 1984 for a recent review). Although true flat-spectrum sources are relatively rare among T Tauri stars, the prototype of the class—T Tauri itself—is such an object. The average T Tauri star typically has a spectral energy distribution which is approximately a power law in the infrared with an index n between the extremes of 4/3 and 0 (see Rydgren et al. 1984, Rucinski 1985, Rydgren and Zak 1987).

The goal of the present paper is fairly modest. By spectral modeling we wish to demonstrate explicitly that the infrared photons of flat-spectrum T Tauri stars can be explained in terms of the thermal emission from disks that have the temperature distribution of equation (3). Our spectral decompositions provide estimates of the relative magnitudes of the intrinsic luminosities of the stars and their disks. By examining how the emission becomes optically thin at submillimeter and millimeter wavelengths, we can place additional limits on the masses and radii of the disks. Finally, we speculate on the physical mechanism by which (active) nebular disks might acquire temperature distributions that are shallower than the classical result, equation (2).

Before we begin, we should point out that our analysis is based on the assumption that the disks are *spatially flat and thin*. The temperature distribution in the disk needed to fit the observations can be used in an *a posteriori* fashion to check the validity of this assumption, namely that the vertical scale height,

$$H \equiv v_T/\Omega , \qquad (4)$$

is much less than the axial distance ϖ from the central star. In the above equation, $v_T = (kT/m)^{1/2}$ is the thermal speed of the gas, and Ω is the local angular velocity. Because of settling, the dust is likely to occupy an even thinner layer than the gas, and the criterion $H \ll \varpi$ is a sufficient, but not necessary, condition for our assumption of a spatially thin disk to be valid.

In Paper I, we mentioned the possibility (suggested by B. G. Elmegreen [1985, private communication]) that reprocessing of stellar photons by a severely flared disk could produce a flat-spectrum infrared source. Kenyon and Hartmann (1987, hereafter KH) have pursued this possibility in more detail and have pointed out that the effective surface for reprocessing stellar photons (basically, where photons of wavelength $\lambda = 1$ μm reach optical depth $\tau_\lambda = 1$) may lie several vertical scale heights above the midplane of the disk $z = 0$. In extreme cases, this effect might modify the radial temperature gradient from equation (2) to equation (3), *without the need to invoke any source of intrinsic luminosity in the disk*.

Apart from minor differences, the formal modeling technique used in the present paper (see also Paper I) is equivalent (for wavelengths that are optically thick in emission) to the method used by KH; we part company with them only in the interpretation of the physical cause of the anomalous radial temperature gradient. In our picture, the disk always reprocesses (only) 25% of the stellar luminosity (see Adams and Shu 1986 and the Appendix to this paper); any additional disk luminosity is then attributed to intrinsic sources. However, it is possible that some fraction of this "intrinsic" luminosity (which we denote as L_D, see below) is actually due to reprocessed stellar photons *in addition to those intercepted by a flat disk*.

However, it is our belief that KH overestimate the efficacy of the flaring mechanism because of the tendency for dust gains to settle from many vertical scale heights (see, e.g., Weidenschilling 1980, 1984, Wetherill 1980) on time scales short (thousands of years) compared to the expected lifetime of the T Tauri stage (10^5–10^6 yr). Convection could potentially keep the dust stirred up (Lin and Papaloizou 1985), but a flared disk vigorously heated by stellar radiation from *above*, with no internal heat flux, should become vertically isothermal and not be unstable to convection. Moreover, convective levitation cannot work beyond a height where the (downward) drift velocity of the dust v_d, relative to the gas, exceeds the latter's (upward and downward) convective velocity v_c. Magnetic fields, if they lay entirely parallel to the x-y plane, could keep charged dust grains (and gas particles) suspended vertically, but such a configuration is Rayleigh-Taylor unstable (Parker 1966, Shu 1974). The magnetic field will buckle and develop a vertical component that will allow the dust grains to slide along the field and drift to the midplane. Thus, for sources without residual infall (see Paper I and § IIIc), we consider it unlikely that appreciable amounts of dust could be kept at vertical distances comparable to the radius—which is necessary in order for a large fraction of the stellar photons to be reprocessed by the disk into the mid- and far-infrared. It is conceivable that stellar winds might "ruffle" dust grains to great heights, but such an explanation would probably require fine-tuning to make the resultant reprocessing yield power-law spectral energy distributions. With this basic underlying philosophy, we start our analysis.

II. THEORETICAL FORMULATION

a) Basic Assumptions

To make models for the spectral energy distribution of T Tauri stars and their disks, we adopt the following simplifying assumptions:

1. We assume that the nebular disk is axisymmetric, perfectly flat, and located in the equatorial plane of the star (as defined by the angular momentum vector). Warps of a disk in a pure Keplerian force field can be maintained if they are appropriately set up initially; however, the presence of any appreciable self-gravity in the disk will cause the warps to propagate as bending waves to the edges where they tend to damp (Hunter and Toomre 1969). Bending waves resonantly forced by a nearby companion in an inclined orbit could keep the disk warped for long periods of time (Shu, Cuzzi, and Lissauer 1983), but, again, we consider it unlikely that the bent shape would almost always work out to yield power-law spectral energy distributions.
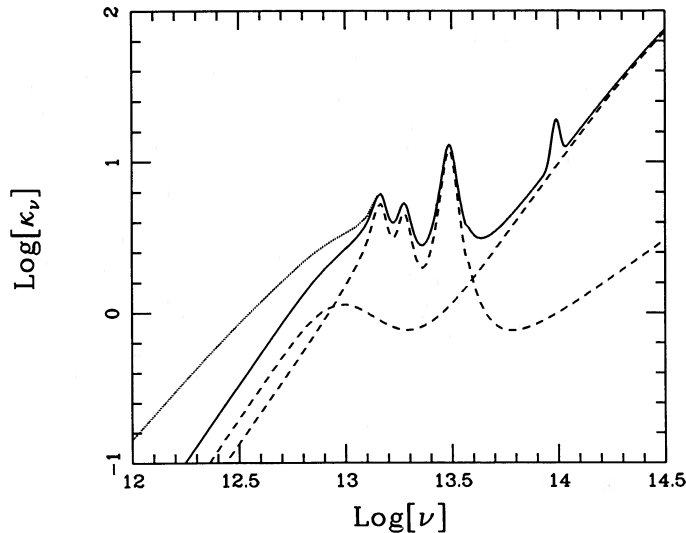
FIG. 1.—Frequency-dependent dust grain opacity in cgs units. The solid line shows the "standard" profile, including the contributions from silicates and graphite, (as shown separately by the dashed lines), and a water ice feature at 3.1 μm; notice that $\kappa_\nu \propto \nu^2$ at low frequencies. The dotted curve shows an alternate opacity profile with $\kappa_\nu \propto \nu^{1.5}$ at low frequencies.

2. Unless explicitly stated otherwise, we assume that the gas opacity in the disk has sufficiently large values to keep the dust-free zone near the star optically thick. The low-temperature opacity tables of Alexander, Johnson, and Rypma (1983) allow us to estimate that this assumption is likely to be valid provided that the surface density Σ is greater than $\sim 10^3$ g cm^{-3} in the regions where the disk temperature exceeds 1500 K.

3. We assume that the infrared dust opacities in the disk have interstellar values close to those computed by Draine and Lee (1984). This allows us to ignore the effects of scattering, i.e., to adopt the approximation that the dust grains are purely absorbing (see Adams and Shu 1985, 1986). Although the opacity is fairly well determined in the near-and mid-infrared, there is considerable uncertainty in the behavior of κ_ν at submillimeter and millimeter wavelengths (see the discussion of Hildebrand 1983). We shall evaluate the sensitivity of our derived model parameters to the adoption of a specific profile for κ_ν by considering the two different laws displayed in Figure 1. The solid and dashed curves in the figure differ in that the former assumes $\kappa_\nu \propto \nu^2$ at low frequencies, while the latter assumes $\kappa_\nu \propto \nu^{1.5}$. The precise values assumed for κ_ν at the shorter wavelengths are unimportant because the radiation from the disks probably remains optically thick until $\sim 100 \mu$m (see § III). Grain agglomeration in the disk will not affect the assumed opacities at longer wavelengths unless the grain sizes become comparable to those wavelengths.

4. For convenience in doing the radiative transfer (see below), we assume that the disk is isothermal *vertically*, although the disk temperature T_D does vary with the axial distance ϖ from the central star. At (short) wavelengths where the radiation from the disk comes from optically thick layers, this assumption results in values for T_D that correspond to the local *effective temperature*. The optically thin radiation at low frequencies contains contribution from everywhere in the disk, including the midplane where the actual material may be appreciably hotter (if the intrinsic flux through the disk is

nonzero) than in the surface layers (where the infrared data determine the distribution of T_D). Thus, our isothermal assumption underestimates the low-frequency emission for a disk of given mass, and overestimates the mass given fixed data points for the submillimeter and millimeter thermal emission. The overestimate of mass will not be large if most of the contribution to the radiation field comes from the outer (i.e., large ϖ) portions of the disk, where the verticle structure *is* likely to be more nearly isothermal (because of lower Rosseland mean optical depths).

5. An implicit assumption contained in our method is that the dust grains reradiate all absorbed photons by acquiring a steady state equilibrium temperature T_D; thus, we have ignored the effect of very small particles or polycyclic aromatic hydrocarbons (PAHs) (see, e.g., Cohen, Tielens, and Allamandola 1985) in our calculations. Since T Tauri stars generally have ultraviolet excesses as well as infrared excesses (see, e.g., the review of Bertout 1987), and since ultraviolet photons are believed to be a source of nonequilibrium excitation for small grains or PAH particles (see Sellgren 1984, Leger and Puget 1984, and Allamandola, Tielens, and Barker 1985), there could be additional near- and mid-infrared radiation that is not adequately modeled by our naive treatment.

b) Formal Solution of the Radiative Transfer Problem

Since the disk is assumed to be spatially thin, any ray passing through the disk (except for the single ray in the direction exactly along the midplane of the disk) will probe only a single radius ϖ. With the further approximation that the disk is isothermal in the vertical direction, the radiative transfer equation can be easily integrated to obtain the monochromatic specific intensity,

$$I_\nu(\varpi, \theta) = B_\nu[T_D(\varpi)]\{1 - \exp[-\tau_\nu^D(\varpi)/\cos \theta]\}, \quad (5)$$

where B_ν is the Planck function and $\tau_\nu^D(\varpi)/\cos \theta$ is the *slant* optical depth through the disk at the radius ϖ for the viewing direction θ. The *normal* optical depth is given by

$$\tau_\nu^D(\varpi) \equiv \kappa_\nu \Sigma(\varpi), \quad (6)$$

where Σ is the disk surface density and κ_ν is the opacity.

The contribution F_ν^D of the entire disk to the radiative flux received by an observer at distance r and polar angle θ can now be computed from

$$4\pi r^2 F_\nu^D = 4g_*(\theta) \cos \theta \exp(-\tau_\nu) \int_{R_*}^{R_D} \pi B_\nu[T_D(\varpi)]$$
$$\times \{1 - \exp[-\tau_\nu^D(\varpi)/\cos \theta]\} 2\pi\varpi \, d\varpi, \quad (7)$$

where R_D is the radius of the disk and $g_*(\theta)$ is the *mean* shadowing function (i.e., occultation of the disk by the star) defined in the Appendix (see also Adams and Shu 1986). (The actual shadowing function depends on the frequency ν of observation, but we ignore this complication.) The factor $\exp(-\tau_\nu)$ represents the selective extinction produced by foreground dust, i.e., *interstellar* material that is not associated with the source. The monochromatic optical depth produced by this foreground material is obtained from the measured visual extinction A_V through the relation,

$$\tau_\nu = \kappa_\nu A_V/\kappa_c, \quad (8)$$

where κ_c is a constant (taken here, for simplicity, to be 200 cm^2 g^{-1}) and where κ_ν is the frequency-dependent dust-grain opacity depicted in Figure 1.

In a similar fashion, the radiant flux received from the star is given through

$$4\pi r^2 F_\nu^* = 4\pi^2 R_*^2 B_\nu(T_*) g_D(\theta) \exp(-\tau_\nu), \qquad (9)$$

where T_* is the (measured) effective temperature of the star, R_* is its radius, and $g_D(\theta)$ is the function which takes into account the shadowing of the star by the disk (see the Appendix). For application to real astronomical sources, we can usually take T_*, A_V, and the observed bolometric system luminosity L_{obs} to be known; all other parameters (e.g., R_* and R_D) must be determined from fitting the observed spectral energy distribution. To perform this operation, we must specify the temperature and surface density distributions, $T_D(\varpi)$ and $\Sigma(\varpi)$, in the nebular disk.

c) Disk Properties

T Tauri stars often have infrared emission in excess of that which can be explained by reprocessing of stellar photons from a spatially flat disk (see, e.g., Paper I); this observational finding leads us to consider active disks which possess intrinsic luminosity. Because the observed spectral energy distributions of T Tauri stars generally exhibit power-law behavior in the infrared, we take the temperature distribution produced by the intrinsic disk luminosity to be a power law in radial distance,

$$T_D(\varpi) = T_{D*} \left(\frac{R_*}{\varpi}\right)^q, \qquad (10)$$

where the coefficient T_{D*} is determined by the intrinsic disk luminosity L_D (see eq. [A7]) and where the temperature index q is left as a free parameter of the theory. At optically thick frequencies, it is easy to show (e.g., Lynden-Bell and Pringle 1974, Beall 1987, Shu, Adams, and Lizano 1987, KH) that the radiant flux from such a disk would follow a power-law distribution, $\nu F_\nu \propto \nu^n$, with

$$n = 4 - \frac{2}{q}. \qquad (11)$$

Thus, flat-spectrum sources (with $n \approx 0$) require a temperature distribution with $q \approx \frac{1}{2}$. In actuality, the disk also reprocesses stellar photons. We assume that a given element on the surface of the disk will radiate both the intrinsic flux corresponding to the intrinsic temperature distribution (eq. [10]) and the energy intercepted from the star, so that the actual disk temperature distribution can be written in terms of the dimensionless variable $u \equiv R_*/\varpi$ as

$$\sigma T_D^4(u) = \left(\frac{L_D}{4\pi R_*^2 \mathscr{D}}\right) u^{4q} + \frac{1}{\pi}\sigma T_*^4[\arcsin u - u(1 - u^2)^{1/2}], \qquad (12)$$

where the quantity $\mathscr{D}$ is of order unity and is defined by equation (A7b). The second term, which arises from disk reprocessing of starlight, is derived in the Appendix (see also Friedjung 1985).

For a disk which satisfies equation (10) and has infinite optical depth (i.e., $M_D \to \infty$), the power law $\nu F_\nu \propto \nu^n$ would hold out to the frequency ν characteristic of the temperature at the outer edge of the disk: $h\nu \sim k T_D(R_D)$. Thus, the outer edge of the disk corresponds to a minimum disk temperature, which in turn leads to a "turnover" frequency—the frequency at which the disk emission begins to depart from the simple power law of index n and (eventually) takes the form appropri-
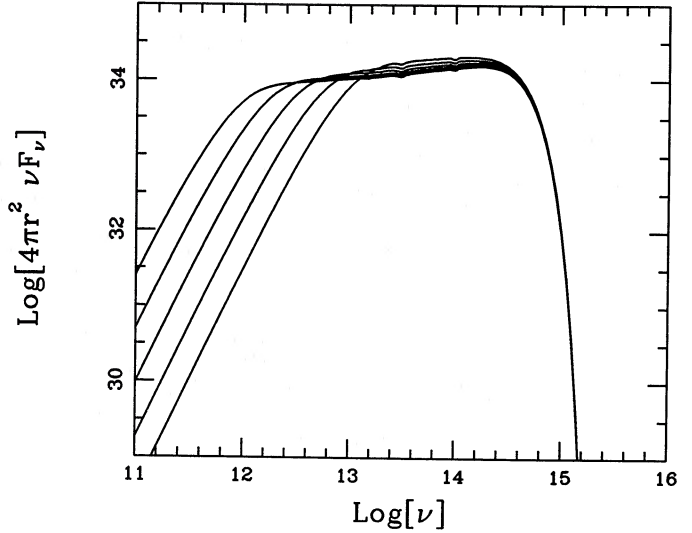

FIG. 2.—Dependence of the emergent spectral energy distribution (cgs units) on the disk outer radius in the optically thick ($M_D \to \infty$) limit. The properties of the star and disk as well as the visual extinction are those of T Tauri in Table 1 with varying outer disk radius $R_D = 10, 31.6, 100, 316, 1000$ AU.

ate for the emission from an arbitrary sum of blackbodies at very low frequencies, $\nu F_\nu \propto \nu^3$. Figure 2 shows the spectral energy distributions for a series of disks with infinite optical depth and varying disk radii R_D. Notice that the "turnover" frequency places a *lower limit* on the disk radius R_D, because the reality of a finite disk mass (and finite optical depth) will cause the rollover from $\nu F_\nu \propto \nu^n$ to occur at even higher frequencies, as shown in Figure 3 for disks with a fixed finite mass and varying outer radius.

Conversely, the observed fact that many disks remain optically thick at wavelengths as long as 100 μm (i.e., have power-law spectra that extend to $\lambda = 100$ μm) can be combined with
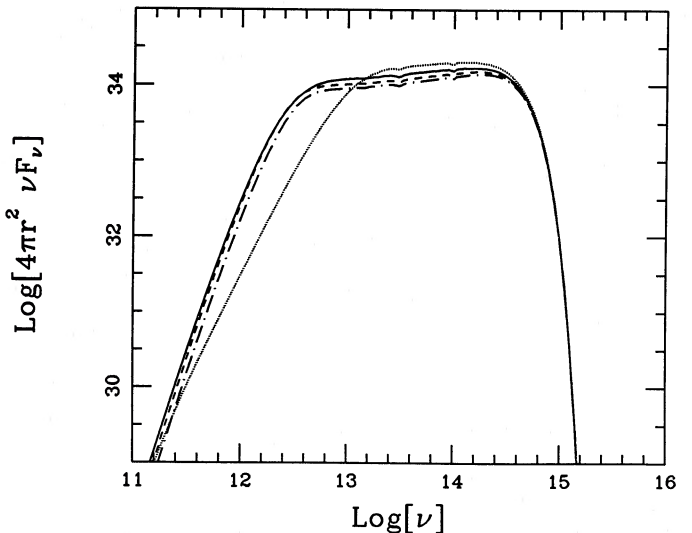

FIG. 3.—Dependence of the emergent spectral energy distribution (cgs units) on the disk outer radius for finite disk mass ($M_D = 0.1$ $M_\odot$). The properties of the star and disk as well as the visual extinction are those of T Tauri in Table 1 with outer disk radii of 10 AU (*dotted curve*), 10^2 AU (*solid curve*), 10^3 AU (*dashed curve*), and 10^4 AU (*dot-dashed curve*).

an estimate (or lower limit) for the disk size R_D to obtain the *minimum mass* of the disk (see, e.g., the use of this idea by Edwards *et al.* 1987). To obtain more precise determinations of the disk mass, it is important to have optically thin submillimeter- or millimeter-wave measurements of the disk's thermal emission (e.g., Beckwith *et al.* 1986, Sargent and Beckwith 1987). To take into account emission at optically thin wavelengths, we adopt a power-law surface density for the disk of form,

$$\Sigma(\varpi) = \Sigma_* \left(\frac{R_*}{\varpi}\right)^p , \qquad (13)$$

where Σ_* is determined by the total mass of the disk M_D and the index p:

$$\Sigma_* = \frac{(2-p)M_D}{2\pi R_*^2 [(R_D/R_*)^{2-p} - 1]} . \qquad (14)$$

In principle, the quantities M_D and p could be taken to be free parameters, to be adjusted to fit the long-wavelength data. However, the sparseness of submillimeter- and millimeter-wave measurements largely vitiates the utility of such an approach. Notice that the optically thin emission at low frequencies (where the Rayleigh-Jeans limit of the Planck function is a good approximation) is proportional to an integral of T_D over the mass distribution of the disk (see eq. [7] in the limit $\tau_\nu^D(\varpi)/\cos\theta \ll 1$). This means that there exists a critical value of the index p, equal to $2 - q$, at which equally spaced logarithmic radial intervals produce equal contributions to the low-frequency emission (i.e., as much radiation is emitted from the inner decade of ϖ as from the outer decade). For $p > 2 - q$, the interior dominates; for $p < 2 - q$, the exterior dominates. However, as long as the value of p is not less than, or much greater than, $2 - q$, the resulting spectral energy distribution will depend only on the total disk mass M_D and will not be very sensitive to the exact value of p (see Fig. 4).

There are no secure arguments which unambiguously determine the surface density distribution and hence the value of p; speculations exist (see, e.g., Quirk 1972 and Paczynski 1978; compare with Lin and Pringle 1987) which suggest that the surface density in a self-gravitating gaseous disk will evolve toward a configuration that keeps the fluid analog of Toomre's (1964) stability parameter,

$$Q \equiv \frac{\Omega v_T}{\pi G \Sigma} , \qquad (15)$$

nearly equal to a constant (of order unity) independent of ϖ. (In eq. [15], we have assumed that the rotation curve is nearly Keplerian so that the epicyclic frequency equals the circular frequency Ω.) For $\Omega \propto \varpi^{-3/2}$ and $v_T \propto T_D^{1/2} \propto \varpi^{-q/2}$, the condition $Q = $ constant yields

$$p = \frac{3+q}{2} . \qquad (16)$$

For $q = \frac{1}{2}$, such a choice of p nearly equals the critical value $(2 - q)$ which leads to all parts of the disk producing equal contributions to the optically thin thermal emission at low frequencies. In this present work, our results are not sensitive to the exact value of p (see Fig. 4), so we adopt the value $p = 7/4$ (in accordance with eq. [16] with $q = 1/2$) for the remainder of this paper.
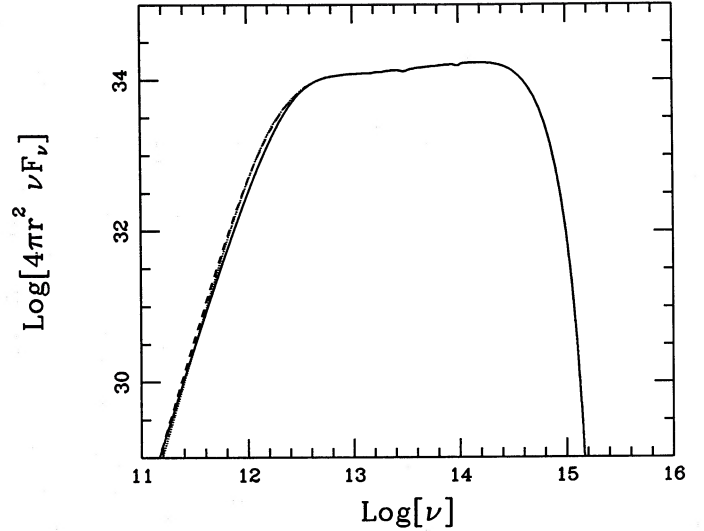

FIG. 4.—Dependence of the emergent spectral energy distribution (cgs units) on the surface density index p. The properties of the star and disk as well as the visual extinction are those of T Tauri in Table 1 with $p = 1.75$ (*solid curve*), 1.0 (*dashed curve*), and 0.0 (*dotted curve*).

The angular dependence of the observed radiant fluxes from the star and disk are given by the shadowing functions $g_D(\theta)$ and $g_*(\theta) \cos\theta$ (see eqs. [7] and [9] and the Appendix). However, as long as the system is *not* viewed from the equatorial direction (where the disk is seen edge-on), the *relative* contributions from the star and disk are not very sensitive to the viewing angle θ (see Fig. 5); hence, we have adopted a "standard" fixed value of $\theta = 45°$ for the remainder of this work. Notice, however, that when the disk has an appreciable intrinsic luminosity, then the inferred bolometric luminosity L of the system can depend fairly sensitively on the observing
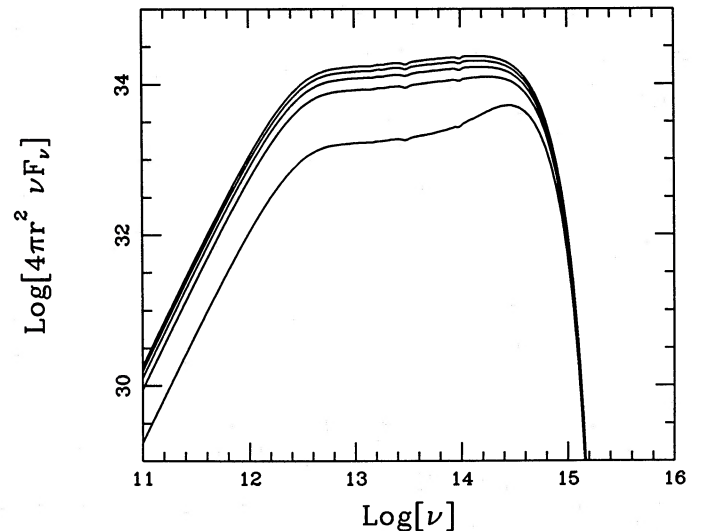

FIG. 5.—Dependence of the emergent spectral energy distribution (cgs units) on the viewing angle θ. The properties of the star and disk as well as the visual extinction are those of T Tauri in Table 1 with $\cos\theta = 1.00, 0.866, 0.707, 0.500, 0.100$. Although the total intrinsic luminosity of the system is 17 $L_\odot$ for all cases shown, the apparent "observed" luminosities $L_{obs} \equiv 4\pi r^2 \int F_\nu^{obs} d\nu$ are 26, 22, 18, 13, and 3.7 $L_\odot$ for the various viewing angles (see text and the Appendix).

angle, especially if one is viewing the system nearly in the equatorial plane. Thus, the inferred luminosity L is not, in general, equal to the "observed" luminosity, $L_{obs} \equiv 4\pi r^2 \int F_\nu^{obs} \, d\nu$, as would be the case for a spherically symmetric system. However, once the viewing angle θ is specified, the observed luminosity L_{obs} can be used to determine the true luminosity of the system L (see the Appendix).

To summarize, we assume that the effective temperature T_* of the central star, the visual extinction A_V, and the bolometric luminosity L_{obs} of the system are known from observations. As described above, the results are not sensitive to the power-law index p for the disk surface density or the viewing angle θ; hence, these quantities are fixed at representative values and do not enter into the following analysis. To calculate the complete spectral energy distribution of a young star with an active disk, we need to specify, in order of descending importance, the following properties of the disk: its intrinsic luminosity L_D, the power-law index q of the disk temperature distribution, the disk radius R_D, and the disk mass M_D. From $L_* = L - L_D$ and T_*, we may obtain the stellar radius R_*. From the spectral slope n in the infrared, we may obtain from equation (11) a good estimate for q. In the limit that the disk is infinitely optically thick, we can use the low-frequency turnover in the $\nu F_\nu \propto \nu^n$ relationship to obtain a lower bound on the disk radius; for most of our models, this radius is taken to be the value of R_D. Although the existing submillimeter observations of T Tauri stars are quite limited, such data can be used, in principle, to determine the mass of the disk M_D.

III. COMPARISON WITH OBSERVATIONS

Using the formulation developed above, we can calculate theoretical spectral energy distributions for T Tauri stars with active disks. For this purpose, we selected a sample of sources with flat spectra, ($n \approx 0$), which represent the most extreme examples of T Tauri stars with infrared excesses. All of the sources that we consider here are in the Taurus molecular cloud complex, which is assumed to have a distance of 140 pc.
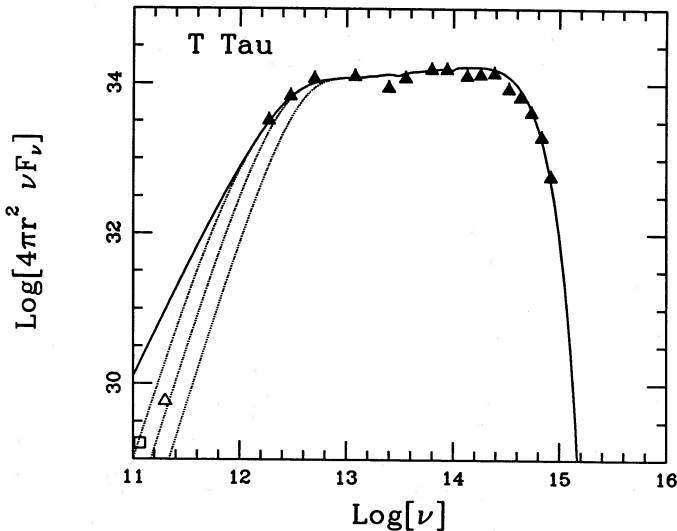
TABLE 1
INPUT PARAMETERS FOR STAR/DISK SYSTEMS

Source	L_{bol} $(L_\odot)$	L_* $(L_\odot)$	L_D $(L_\odot)$	T_* (K)	A_V (mag)	q
T Tau	17.0	5.10	11.9	5105	1.44	0.515
DG Tau	6.10	0.61	5.49	5495	3.00	0.510
DG Tau[a]	6.10	0.61	5.49	3500	3.00	0.510
HL Tau	6.00	1.00	5.00	4000	7.00	0.501
HP Tau	2.30	1.04	1.26	4775	2.32	0.533
ZZ Tau	0.93	0.64	0.29	3230	1.00	0.501
HK Tau	1.00	0.75	0.25	3800	3.42	0.501
Composite	1.50	0.50	1.00	4000	...	0.600

[a] Alternate model with lower spectral temperature to correct for the possible contamination of the stellar spectrum by a hot boundary layer (see text).

Since the spectra of all of these sources are very flat, the corresponding values of the temperature index q required in order to fit the spectral energy distributions are all nearly $\frac{1}{2}$. These values, along with the other specifications of these star/disk systems, are summarized in Table 1. For all the sources considered here, we first use the spectrum of a completely optically thick disk (i.e., the $M_D \to \infty$ limit) to determine the minimum disk radius for the system; we then calculate the spectral energy distributions for finite disk masses of 0.01, 0.1, and 1.0 $M_\odot$. Since these flat-spectrum sources constitute only a small subset ($\sim 10\%$) of all T Tauri stars, we also address the more "typical" case by fitting the composite spectrum of seven "ordinary" T Tauri stars.

a) T Tau

The prototypical young star with a flat infrared spectrum—T Tauri—has a K1 spectral classification (Herbig and Rao 1972), corresponding to an effective photospheric temperature of 5100 K; the visual extinction to the star is 1.4 mag (CK). To fit the spectral energy distribution requires an intrinsic disk luminosity of 11.9 $L_\odot$, which is relatively large in comparison with the intrinsic stellar luminosity of only 5.1 $L_\odot$. Figure 6a
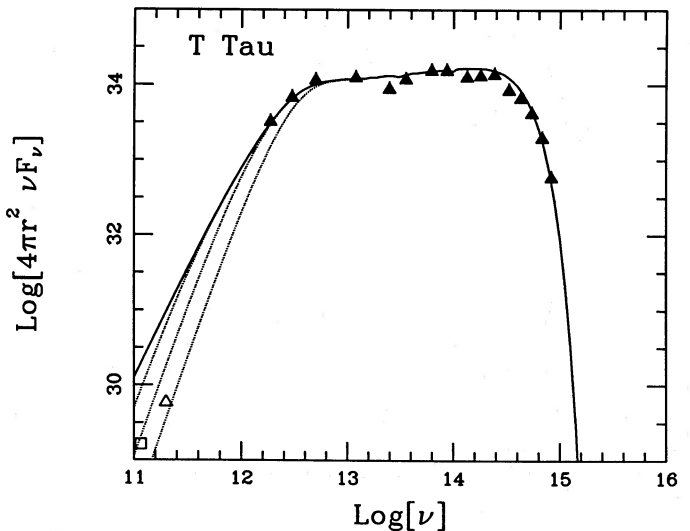

FIG. 6a

FIG. 6b

FIG. 6.—Theoretical and observed spectra of infrared source T Tauri (cgs units). Solid curve shows the spectrum in the optically thick ($M_D \to \infty$) limit; dotted curves show spectra for finite disk masses of 0.01, 0.1, and 1.0 $M_\odot$. The solid triangles are the observed data points, the open triangle is an upper limit to the 1.3 mm flux, and the open square is an upper limit/detection of the 2.6 mm flux. The stellar surface temperature is taken to be 5100 K, with a stellar luminosity of 5.1 $L_\odot$; the disk luminosity is taken to be 11.9 $L_\odot$, with disk radius $R_D = 120$ AU. (a) Spectrum for "standard" opacity profile with $\kappa_\nu \propto \nu^2$ at low frequencies. (b) Spectrum for alternate opacity profile with $\kappa_\nu \propto \nu^{1.5}$ at low frequencies.

shows the theoretical spectral energy distribution for a minimum disk radius of ~ 120 AU, along with observational data taken from Cohen and Schwartz (1976), Rydgren, Strom, and Strom (1976), and from *IRAS*. The open triangle represents an upper limit to the flux at 1.3 mm (Walker, Adams, and Lada 1987), which gives an upper limit to the disk mass of approximately 0.2 $M_\odot$ if $\kappa_\nu \sim \nu^2$ at low frequencies. The open square represents the 2.6 mm continuum flux, which was first measured as an upper limit (Weintraub, Masson, and Zuckerman 1987), and later an actual detection (D. Weintraub, private communication), indicating a disk mass estimate/limit of nearly 1 $M_\odot$. The disk mass estimate/limit becomes ~ 0.02–0.1 $M_\odot$ if we adopt the alternative behavior $\kappa_\nu \sim \nu^{1.5}$ at low frequencies (see Fig. 6b). Similar reductions by about a factor of 10 hold for our other models; consequently, we shall henceforth display only the results for the former assumption.

T Tauri has a companion (see Dyck, Simon, and Zuckerman 1982), and it has been suggested that the observed infrared excess may be produced by this object (e.g., Hanson, Jones, and Lin 1984). However, as illustrated by the rather good agreement between theory and observation shown in Figure 6, the infrared emission from T Tauri must originate from regions with a wide range of temperatures, from 30 K to 5000 K; hence, no photosphere with a *single effective temperature* (i.e., no starlike or planetlike object) can produce the observed infrared excess in T Tauri.

The projected separation of T Tauri and its companion is observed to be ~ 100 AU (Dyck, Simon, and Zuckerman 1982), which is close to the theoretically derived minimum disk radius (120 AU) for this system. Although the agreement may be a coincidence, one intriguing possibility is that the companion has tidally truncated the disk (see, e.g., Lin and Papaloizou 1979). In any case, a closely orbiting companion may drive density waves in the disk of T Tauri (see, e.g., Borderies, Goldreich, and Tremaine 1985, Shu *et al.* 1985), but the total energy dissipation from such driven waves is unlikely to produce a flat spectrum source because the required resonances in the deep interior of the disk will either be weak or absent.

b) DG Tau

The star DG Tau generally exhibits a continuous spectrum (with no absorption lines), although in one case it has been classified as a G star (see Herbig and Rao 1972), implying a surface temperature of 5500 K. In addition, the visual extinction to this source is not well measured. If we adopt a value of 3.0 mag for A_V, our models require an intrinsic disk luminosity of 5.5 $L_\odot$, leaving only 0.6 $L_\odot$ for the intrinsic stellar luminosity (Fig. 7). This low stellar luminosity and high surface temperature would place DG Tau nearly on the zero-age main sequence, which is not a reasonable result given the extreme ultraviolet excess of DG Tau, which probably indicates the presence of a strong boundary layer and therefore considerable disk accretion (see Bertout, Basri, and Bouvier 1987). The ultraviolet emission from this boundary layer has not been taken into account by our analysis. It is likely that the G star classification for DG Tau is incorrect, possibly because of contamination by the boundary layer, and that the star is intrinsically cooler and more luminous (again, see Bertout, Basri, and Bouvier 1987). The dashed line in Figure 7 shows a spectrum corresponding to $T_* = 3500$ K, with all the other quantities held fixed. In either case, if we use a minimum disk radius of 75 AU, the spectral energy distribution can be reasonably fit to the observations by the procedure of this paper (except for the
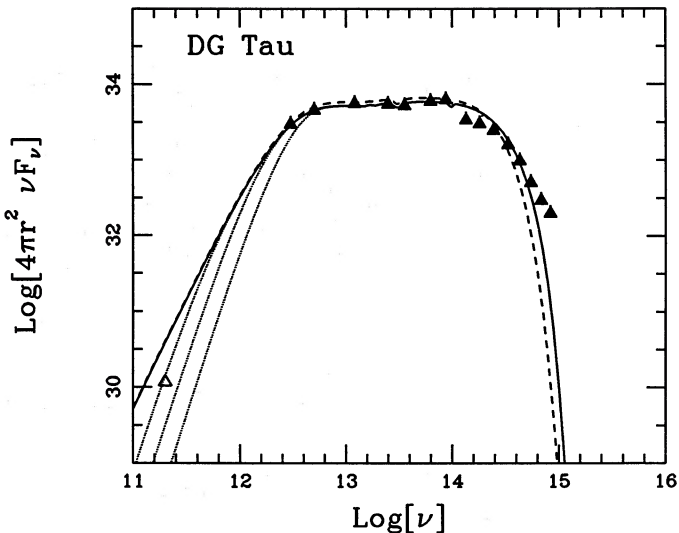

FIG. 7.—Theoretical and observed spectra of infrared source DG Tauri (cgs units). Solid curve shows the spectrum in the optically thick ($M_D \to \infty$) limit for an assumed stellar photospheric temperature of 5495; the dashed curve assumes a cooler stellar surface temperature of 3500 K (see text); dotted curves show spectra for finite disk masses of 0.01, 0.1, and 1.0 $M_\odot$. The stellar luminosity is taken to be 0.6 $L_\odot$, whereas the intrinsic disk luminosity $L_D = 5.5 L_\odot$, with disk radius $R_D = 75$ AU. The solid triangles are the observed data points, whereas the open triangle is an upper limit to the 1.3 mm flux. Notice the extreme excess observed in the UV portion of the spectrum.

ultraviolet excess). The optical and infrared data in Figure 7 are taken from Cohen and Schwartz (1976); Rydgren, Strom, and Strom (1976); and the *IRAS* point source catalog. The open triangle represents an upper limit to the 1.3 mm flux (Walker, Adams, and Lada 1987), which in turn implies an upper limit to the disk mass of ~ 1.0 $M_\odot$ if $\kappa_\nu \propto \nu^2$ at low frequencies.

c) HL Tau

The infrared source HL Tau is extreme in several ways. First, the visual extinction to the source is large for an optically visible object, approximately 7 mag (Cohen 1983), making HL Tau the only T Tauri star with both a detectable silicate absorption feature at 9.7 μm and an ice absorption feature at 3.1 μm (Cohen 1975). The star normally exhibits a continuous spectrum (i.e., no absorption lines), although it has been classified as a K7 star in one instance (see CK). If we accept this classification, the effective temperature $T_* = 4000$ K. The infrared excess then requires an intrinsic disk luminosity of 5.0 $L_\odot$, leaving a stellar luminosity of only 1.0 $L_\odot$. Using a minimum radius of 100 AU, we can fit the spectrum as shown in Figure 8. The short wavelength data ($\lambda \leq 10$ μm) come from the catalog of Rydgren *et al.* 1984, which in turn are a compendium from Cohen and Schwartz (1976), Rydgren, Strom, and Strom (1976), Rydgren and Vrba (1981, 1983), Strom, Strom, and Vrba (1976), and Cohen (1980). For $\lambda \geq 20$ μm, the data are from KAO measurements (Cohen 1983) and from the *IRAS* point source catalog. Since the *IRAS* beam includes both HL Tau and XZ Tau, the measured flux must be divided between the two sources; this is done under the assumption that each source contributes a constant fraction of the total flux, with the fraction determined by the ratio of the resolvable fluxes from the sources (Martin Cohen, private communication).
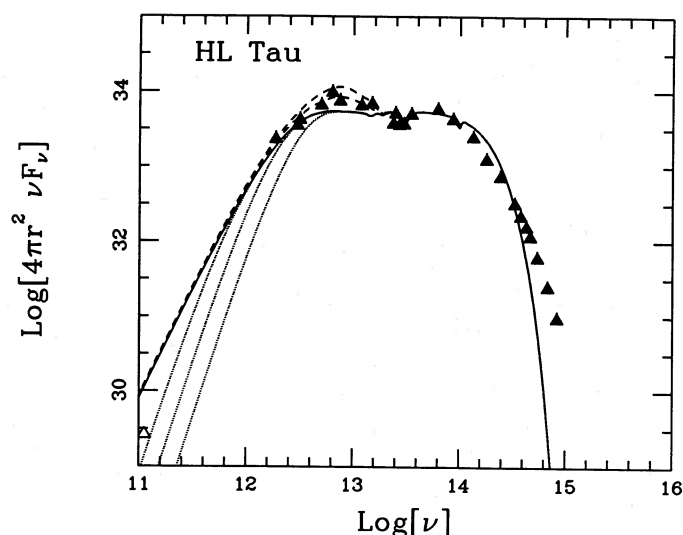
FIG. 8.—Theoretical and observed spectra of infrared source HL Tauri (cgs units). Solid curve shows the spectrum in the optically thick $(M_D \to \infty)$ limit; dotted curves show spectra for finite disk masses of 0.01, 0.1, and $1.0 M_\odot$. The dashed curves show the additional flux contribution of a residual infalling dust envelope surrounding the entire star/disk system for covering fractions of 0.5 and 1.0. The stellar luminosity is 1.0 $L_\odot$ with an effective surface temperature of 4000 K; the disk luminosity is 5.0 $L_\odot$, with disk radius $R_D = 100$ AU. The solid *and* open triangles both represent actual measurements in this case; again, notice the large UV excess in the data.

As illustrated by the solid line in Figure 8, a simple star/disk system does not produce enough luminosity in the far-infrared to account for the observed emission of HL Tau. However, the large value of A_V for this source implies that a significant fraction of the intrinsic luminosity will be absorbed (and presumably reradiated at longer wavelengths) by the circumstellar material responsible for the extinction. To take this into account, we have constructed a model for an optically thin spherical dust shell surrounding the entire star/disk system (see Paper I for a complete description of the method). The dust shell is assumed to have a density distribution of the form $\rho \propto r^{-2}$ and a temperature distribution of the form $T \propto r^{-1/3}$. Using the constraints that the total extinction produced by the dust shell must equal the observed value and that the total energy radiated by the shell must equal the amount of energy absorbed from the central source, the only remaining parameter of the theory is the inner radius of the dust shell. For HL Tau, this radius is taken to be 8×10^{14} cm, which is near the outer radius of the disk. We also allow the covering fraction of the shell material to be less than unity; this follows from our interpretation that the dust shell results from residual infall (see also the arguments in Shu, Adams, and Lizano 1987). This infall should take place primarily along an equatorial belt, if we assume that the polar regions have been evacuated by a bipolar outflow. The resulting spectra are shown as dashed curves in Figure 8 for covering fractions of 1.0 and 0.5. Notice that the total amount of radiation absorbed and reradiated by the dust shell is smaller than one might expect for $A_V = 7$, because much of the intrinsic luminosity of the system is radiated by the disk at long wavelengths where the photon absorption cross-section of interstellar dust grains is small.

The possibility that HL Tau has a circumstellar disk was first suggested by Cohen (1983) on the basis of the observed absorption features in the spectrum. Near-infrared imaging of the object (Grasdalen *et al.* 1984) and speckle interferometry

(Beckwith *et al.* 1984) confirmed the presence of a flattened distribution of light scattering particles, with the estimates for the total mass in scattering dust grains of $\sim 10^{-7} M_\odot$. Measurements of the 2.7 mm continuum radiation from the source (Beckwith *et al.* 1986) found a much greater mass for the dust in thermal *emission*, with the exact result dependent on the assumed emissivity and temperature of the grains. Their datum is plotted as an open triangle in Figure 8; our model for the temperature distribution combined with a v^2 emissivity law at low frequencies implies a total disk mass (including gas and dust) of $\sim 2 M_\odot$. A $v^{1.5}$ emissivity law (see Fig. 1) would lower the deduced mass by approximately a factor of 10, in rough agreement with results derived from recent ^{13}CO observations of HL Tau (Sargent and Beckwith 1987); however, absolute radiometer measurements of the thermal emissivity from dust suggests that the v^2 law may be a better approximation for interstellar grains (A. Lange 1987, private communication).

In a review of the situation concerning the various discrepant mass estimates, Shu, Adams, and Lizano (1987) proposed that the earlier scattering and absorption measurements referred to the residual infalling material surrounding the central source and not to the true disk. This interpretation is supported by the present calculations. The amount of dust contained within 140 AU (1″) of our model of the infalling shell in Figure 8 is 1×10^{-6} and $2 \times 10^{-6} M_\odot$, respectively, for a covering fraction of 0.5 and 1, and appears roughly consistent with the scattering and absorption measurements. (Notice that Fig. 8 reproduces the depth of the silicate absorption feature.)

d) HP Tau

The observed and theoretical spectra of HP Tau are shown in Figure 9, with data taken from Rydgren and Vrba (1983)
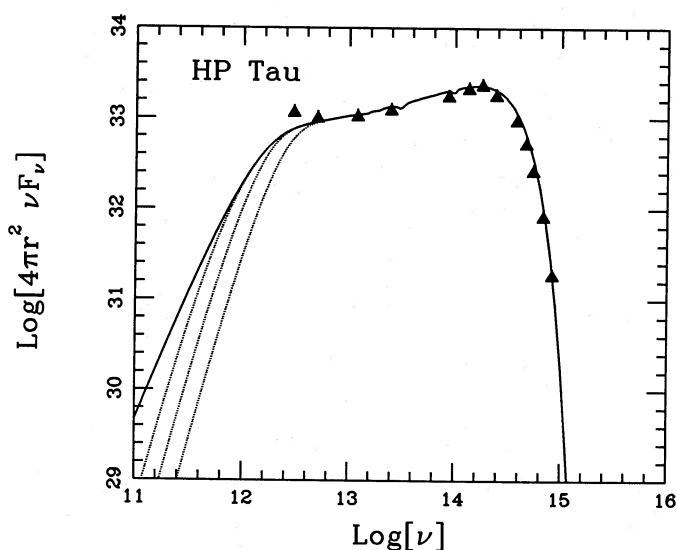

FIG. 9.—Theoretical and observed spectra of infrared source HP Tauri (cgs units). Solid curve shows the spectrum in the optically thick $(M_D \to \infty)$ limit; dotted curves show spectra for finite disk masses of 0.01, 0.1, and $1.0 M_\odot$. The stellar surface temperature is taken to be 4780 K, with a stellar luminosity of 1.0 $L_\odot$; the intrinsic disk luminoity is 1.3 $L_\odot$, with disk radius $R_D = 100$ AU. The solid triangles are the observed data points. The apparent lack of UV excess is misleading in this plot because the stellar atmosphere has been modeled as a blackbody, an incorrect procedure unless the star has an active chromosphere (with a modest UV excess in comparison with a *normal star*) that combines with the photosphere to mimic an isothermal atmosphere (i.e., one without a deep temperature minimum).

and *IRAS*. The star is classified as a K3 star, indicating a surface temperature of 4780 K (CK); the visual extinction to the source is given as 2.3 mag (CK). The intrinsic disk luminosity, 1.3 $L_\odot$, is comparable to that of the star, 1.0 $L_\odot$; thus, this source is less extreme than those discussed above. The estimated minimum disk radius is ~100 AU, although this prediction is not very secure. Notice that the observed 100 μm point falls above the theoretical curve in Figure 9. Although it is possible to obtain a slightly better fit to the far-infrared data by using a flatter disk temperature distribution, this tends to reduce the quality of agreement in the near-infrared (i.e., the *JHKL* points). Since the 100 μm point is probably the most uncertain, we adopt the fit shown in Figure 9.

e) ZZ Tau

The next source that we consider, *ZZ Tau*, has a flat spectrum, but the overall luminosity in the far-infrared is small (0.29 $L_\odot$) compared to that of the star (0.64 $L_\odot$). The star is classified as M4 (Herbig and Rao 1972), implying a surface temperature of 3230 K. Since no value of the visual extinction was found in the literature, we have adopted a value of 1.0 mag, which is typical for T Tauri stars. Using an estimated minimum disk radius of 40 AU, the resulting spectral energy distribution is compared to the observational data in Figure 10, with the data taken from Rydgren and Vrba (1983) and *IRAS*. Notice that the theory predicts too much emission in the 2–10 μm portion of the spectrum. One explanation for this observed absence of disk emission is that there is a hole or gap (perhaps only in opacity rather than in matter) in the inner region of the disk, as illustrated by the dashed curve in Figure 10; this curve assumes that there is no disk emission for radii
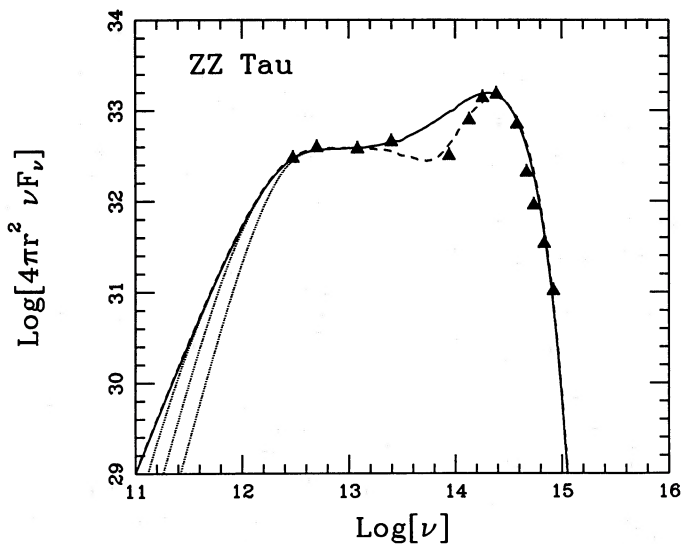
less than 1.5×10^{12} cm = 0.1 AU, which implies a maximum observable disk temperature of 600 K. An alternate explanation for the absence of near-infrared emission in this source is that the *IRAS* (i.e., 12–100 μm) data correspond to emission from a nearby (optically invisible) source. Although this interpretation may be correct for this object (and perhaps others), source confusion will not, in general, produce flat spectra and cannot provide the explanation for all flat spectrum T Tauri stars.

f) HK Tau

The final star that we consider, HK Tau, is very similar to ZZ Tau in that both sources have very flat spectra but relatively low luminosities in the far-infrared. The spectral type of the star has been measured to be M0.5 (CK) and dM0 (Herbig and Rao 1972), implying a surface temperature of ~3800 K; we adopt a visual extinction of 3.4 mag in agreement with the upper limit given in CK. The intrinsic luminosity of the disk, 0.25 $L_\odot$, is again smaller than that of the star, 0.75 $L_\odot$. Using a minimum disk radius of 100 AU, the spectrum can be fit as shown in Figure 11, with the data taken from Rydgren, Schmelz, and Vrba (1982), Rydgren and Vrba (1983), and from *IRAS*. However, it is interesting to notice that the spectra of both HK Tau and ZZ Tau, which have been modeled with disks of relatively low luminosity and viewing angles of 45°, are similar to that of a system with a more luminous disk viewed nearly edge-on (see Fig. 5).

g) Composite Spectrum of Seven T Tauri Stars

The sources that we have considered above are among the most extreme T Tauri stars. More "typical" stars have infrared

FIG. 10

FIG. 11

FIG. 10.—Theoretical and observed spectra of infrared source ZZ Tauri (cgs units). Solid curve shows the spectrum in the optically thick ($M_D \to \infty$) limit; dotted curves show spectra for finite disk masses of 0.01, 0.1, and 1.0 $M_\odot$. The dashed curve shows the effect of removing the inner ($\varpi \leq 0.1$ AU) region of the disk. Here, the stellar surface temperature is 3230 K, with stellar luminosity of 0.64 $L_\odot$, an intrinsic disk luminosity of 0.29 $L_\odot$, and a disk radius $R_D = 40$ AU. The solid triangles are the observed data points. The apparent lack of a UV excess is misleading in this plot because the stellar atmosphere has been modeled as a blackbody, an incorrect procedure unless the star has an active chromosphere (with a modest UV excess in comparison with a *normal star*) that combines with the photosphere to mimic an isothermal atmosphere (i.e., one without a deep temperature minimum).

FIG. 11.—Theoretical and observed spectra of infrared source HK Tauri (cgs units). Solid curve shows the spectrum in the optically thick ($M_D \to \infty$) limit; dotted curves show spectra for finite disk masses of 0.01, 0.1, and 1.0 $M_\odot$. The intrinsic disk luminosity is taken to be 0.25 $L_\odot$ with disk radius $R_D = 100$ AU, whereas the stellar luminosity is 0.75 $L_\odot$ with a surface temperature of 3800 K. The solid triangles are the observed data points. The apparent lack of a UV excess is misleading in this plot because the stellar atmosphere has been modeled as a blackbody, an incorrect procedure unless the star has an active chromosphere (with a modest UV excess in comparison with a *normal star*) that combines with the photosphere to mimic an isothermal atmosphere (i.e., one without a deep temperature minimum).
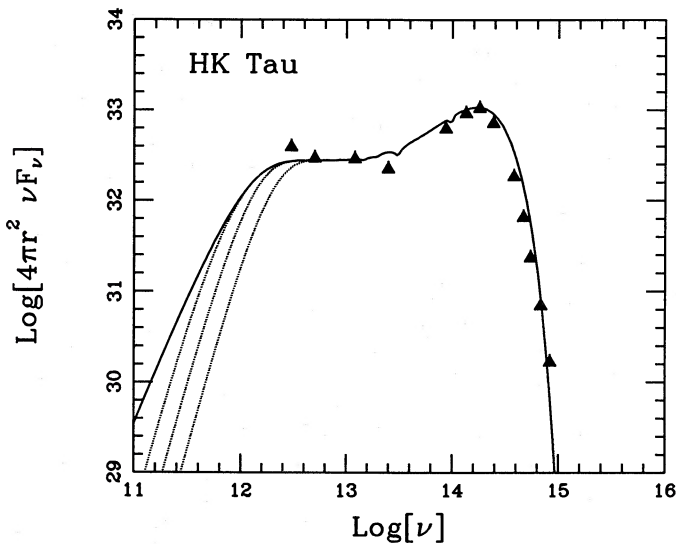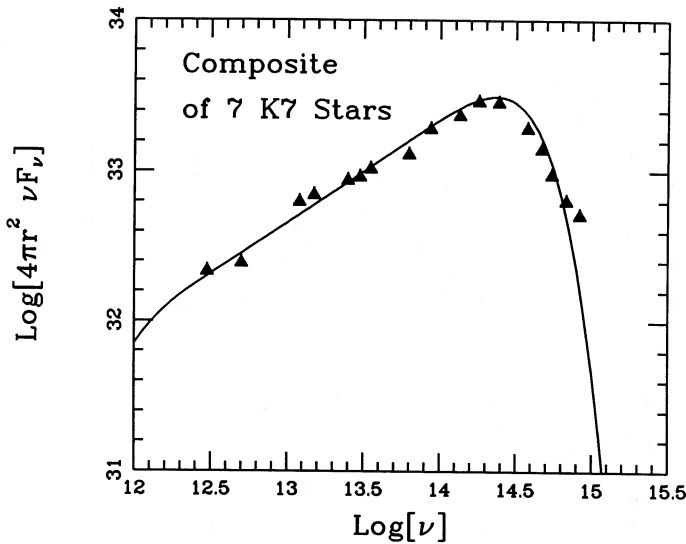
FIG. 12.—Composite spectral energy distribution of seven T Tauri stars: DK Tau, GI Tau, GK Tau, CI Tau, UY Aur, BP Tau, and DL Tau (cgs units). The individual data sets have been *dereddened* and averaged together to produce the composite spectrum shown by the solid triangles. The solid curve shows the theoretical spectrum for a K7 star ($T_* = 4000$ K) with a stellar luminosity $L_* = 0.5 \, L_\odot$ and a disk with temperature index $q = 0.6$ and intrinsic luminosity $L_D = 1.0 \, L_\odot$. Notice the UV excess that may be an indicator of boundary-layer activity.

TABLE 2

OUTPUT PARAMETERS FOR STAR/DISK SYSTEMS

Source	M_* ($M_\odot$)	R_* (10^{11} cm)	M_D ($M_\odot$)	M_Q ($M_\odot$)	$R_{D\min}$ (AU)
T Tau	1.80	2.1	0.2	1.3	120
DG Tau	0.95	0.62	1.0	0.78	75
DG Tau[a]	0.40	1.5	1.0	0.50	75
HL Tau	0.80	1.5	2.0	0.76	100
HP Tau	1.25	1.1	...	0.78	(100)
ZZ Tau	0.30	1.8	...	0.26	40
HK Tau	0.50	1.4	...	0.42	(100)
Composite	0.75	1.1	...	0.52	(100)

[a] Alternate model with lower spectral temperature to correct for the possible contamination of the stellar spectrum by a hot boundary layer (see text).

excesses with steeper spectral slopes. Rydgren and Zak (1987) have produced a composite spectral energy distribution for the infrared excesses in T Tauri stars, which indicates an average spectral index of $n = 0.75$, whereas Rucinski (1985) advocates $n = 1.0$ as the representative value. To demonstrate that the theory developed here adequately explains the more typical cases, we have compiled a composite spectrum of seven T Tauri stars with a procedure similar to that of Rydgren and Zak (1987). However, we limit our sample to stars of a single spectral type, K7, including five from the Rydgren and Zak sample (DK Tau, GI Tau, GK Tau, CI Tau, and UY Aur) and two other similar stars (BP Tau and DL Tau). We use the *UBVRI* and *JHKL* data points from the catalog of Rydgren et al. 1984, which are in turn taken from Rydgren and Vrba (1981), Rydgren, Schmelz, and Vrba (1982), Rydgren and Vrba (1983), and *IRAS* data in the far-infrared. The intermediate wavelength data (4.8–20 μm) are taken from Cohen (1973), Cohen and Schwartz (1976), Elias (1978), Grasdalen (unpublished), Rydgren, Strom, and Strom (1976), and Vrba and Rydgren (unpublished). The spectral energy distributions are corrected for interstellar extinction using the values of A_V given by CK and then averaged together to produce the composite spectral energy distribution shown in Figure 12. The spectrum can be fitted with a theoretical model using a stellar luminosity of 0.5 $L_\odot$ and an intinsic disk luminosity of 1.0 $L_\odot$. The surface temperature of the composite star is taken to be 4000 K, in accordance with the K7 spectral classification. The temperature index q must be 0.6 in order to produce the mean spectral slope of $n = 0.67$.

IV. RESULTS AND INTERPRETATION

a) Stellar Properties

A byproduct of fitting the observed T Tauri spectra is a formal determination of the stellar properties, in particular the stellar luminosity L_* and the stellar radius R_* (see Tables 1 and 2). These determinations depend on the assumption that the spectral type of the star is accurately known (and not affected, e.g., by the presence of a boundary layer or strong chromospheric veiling) and that the disk is spatially thin (and does not, therefore, reprocess more than $\frac{1}{4}$ of the stellar photons). Given these two assumptions, our models require appreciable intrinsic disk luminosity in order to fit the observations of most flat-spectrum T Tauri stars; consequently, our derived values for L_* and R_* differ substantially from those obtained under the assumption that all of the bolometric luminosity of the system originates in the star. The actual corrections needed (e.g., for proper placement on the Hertzsprung-Russell diagram of the vast majority of T Tauri stars) are probably not as severe as indicated by our models because the effects of disk flaring will result in a greater fraction of the intrinsic luminosity being attributed to the central stars (KH). In particular, the infrared excesses of the less extreme sources ZZ Tau and HK Tau *might* be explained by flaring passive disks. Nevertheless, disk flaring cannot plausibly account for the infrared spectral energy distributions of the most extreme examples considered in this paper (T Tau, DG Tau, HL Tau), and these systems will require substantial revisions of their conventionally abscribed properties. The revisions may not be exactly as described in Tables 1 and 2 because of possible ambiguities in the assignment of accurate spectral types and the uncertainties in the visual extinctions A_V. It is precisely these stars where the ultraviolet excesses are also most extreme, indicating that star-disk interactions (perhaps in the form of a boundary layer; see Bertout, Basri, and Bouvier 1987) may be affecting the observed formation of the absorption lines and slopes of the underlying stellar continua.

If we blindly assume that the assigned spectral types *are* accurate, we may use the corresponding effective temperature T_*, combined with the derived stellar luminosity L_*, to derive an inferred stellar mass M_* by comparison with published evolutionary tracks for pre–main-sequence stars (e.g., Iben 1965). Mass determinations by this method are indicated in the second column of Table 2. Unfortunately, these mass determinations may still be flawed because the theoretical pre–main-sequence tracks themselves may need to be revised in order to properly account for the presence of mass accretion from the disk onto the star through a boundary layer. Conventional tracks are usually calculated under the assumption that the star is spherical and isolated from its environment; this may be a poor approximation in the case of stars surrounded by very

active disks. However, for the special case of stars that are fully convective and, therefore, have photospheric temperatures T_* at the Hayashi limit (Hayashi, Hoshi, and Sugimoto 1962), the inferred stellar masses are relatively insensitive to everything except the derived value for T_*. Although some calculations including the effects of disk accretion have been attempted (e.g., Mercer-Smith, Cameron, and Epstein 1984, Stringfellow 1987), these calculations generally adopt ad hoc prescriptions to determine the specific entropy of the material that is accreted from the disk onto the star through a boundary layer. Additional analysis of this problem would be very valuable.

b) Disk Properties

Although attempts have been made to explain the spectra of sources with infrared excesses that invoke models of spherical dust shells surrounding the stars (see Wolfire and Churchwell 1987, Rowan-Robinson et al. 1986), such models are not well motivated in the case of optically revealed T Tauri stars (see the discussion of Shu, Adams, and Lizano 1987). In our view, spatially flat disks are necessary in these objects to explain the combination of low visual extinction (as measured by reddening as well as by the general lack of appreciable ice and silicate absorption features) and large infrared emission. In our models, the physical properties of the disk, in particular, the disk luminosity L_D and the intrinsic disk temperature distribution T_D, are determined directly from fitting the observed spectral energy distributions.

Our results suggest that most flat-spectrum T Tauri stars must have *active* disks, with intrinsic disk luminosities often greater than the stellar luminosities. In addition, the flatness ($n \approx 0$) of the observed spectral energy distributions can be understood only if the disk temperature profile is shallower (i.e., $T_D \sim \varpi^{-1/2}$) than that of a classical viscous accretion disk ($T_D \sim \varpi^{-3/4}$). Notice that the spectral index of the "typical" T Tauri star (see § III*g*) is almost exactly halfway between the extreme values of $n = 4/3$ and $n = 0$; spectral slopes in this intermediate range may be explained by the reprocessing of stellar photons from a flared disk (KH). However, the large infrared excesses of the extreme flatspectrum sources (and some sources with steeper spectra) cannot be produced by a flared disk unless the disk reprocessing surface is significantly above the scale height H of the gas (and this effect is highly unlikely because of dust settling). Thus, the flaring effect considered by KH probably does contribute to the infrared excess of the "typical" T Tauri star, but does not fully explain the large infrared excesses found in many sources.

Limits on the minimum sizes of the required disks can be set by considering model disks that are optically thick at every observed frequency (see § II above). The resulting values for $R_{D \, min}$ (see Table 2) are roughly consistent with the sizes expected from the theory of the gravitational collapse of rotating molecular cloud cores (Terebey, Shu, and Cassen 1984; see also the discussion of Paper I), especially if we allow for some spreading of the disks due to internal redistribution of mass and angular momentum.

The masses of the disks in these systems can also be estimated through spectral modeling. If data at submillimeter and millimeter wavelength exist, the disk mass can be determined directly by comparing the observed continuum emission with that expected from the theoretical models described above. Unfortunately, little data is currently available; we have (crude) estimates for the disk masses for T Tauri ($M_D \approx 0.2$ $M_\odot$) and HL Tau ($M_D \approx 2$ $M_\odot$) and an upper limit for DG

Tauri ($M_D < 1.0 \, M_\odot$). As discussed in the preceding section, these values are sensitive to the exact dust grain opacity at submillimeter wavelengths, which is somewhat poorly known at present. However, if enough data become available to unambiguously determine the spectral slope at submillimeter wavelengths, the opacity dependence can be separated out and improved mass estimates can be made. With the present uncertainty in the opacity and the sparseness of submillimeter data, the current disk mass estimates should be regarded as somewhat tentative. In the absence of submillimeter data, another limit on the disk mass can be placed by requiring that the disk be gravitationally stable against all axisymmetric perturbations; the maximum disk mass M_Q can then be found by setting $Q = 1$ in equation (15) and using the result to determine a critical surface density Σ which can be integrated over the surface of the disk to obtain the critical disk mass M_Q:

$$M_Q \equiv \int_{R_*}^{R_D} \frac{\Omega v_T}{\pi G} \, 2\pi\varpi \, d\varpi \, . \tag{17}$$

Since the resulting values of M_Q (maximum mass for a stable disk) are not much larger than the inferred masses of T Tauri stars[1] (see Table 2), the rotation curves of the disks should be very nearly Keplerian at the large radii where the far-infrared emission originates. The possibility mentioned in Paper I, that the flat-spectrum sources with $T_D \propto \varpi^{-1/2}$ might owe their origin to viscous accretion in a non-Keplerian field of rotation (in particular, a disk with a *flat* rotation curve), is therefore quite unlikely.

We can also use the deduced disk temperature distribution and rotation curve to estimate the scale height H in the disk and, thus, verify our assumption that $H \ll \varpi$. For a disk which is not strongly unstable (i.e., Q is not $\ll 1$, or M_D is not $\gg M_Q$), the gaseous scale height is given by equation (4), and the condition $H \ll \varpi$ is equivalent to the condition $v_T \ll \Omega\varpi$. Consider, for example, the case for our models of T Tauri: just beyond the surface of the star (where the hydrogen gas can be assumed to be primarily atomic), $H/\varpi = 0.017$; at a radius of 1 AU (where the hydrogen gas can be assumed to be molecular), $H/\varpi = 0.031$; and at the outer edge of the disk (where the hydrogen gas can again be assumed to be molecular), $H/\varpi = 0.099$. Such ratios are typical of all of our models, justifying *a posteriori* our treatment of the disks as very flat structures.

An indirect argument exists for the disks around T Tauri stars not being overly thick. For example, if a disk has an aspect ratio of 2:1 (which is necessary to reprocess a majority of the stellar photons), then it is just as likely for an arbitrarily situated observer to view the star *through* the disk as from above the disk. Statistically, then, there should be as many heavily obscured sources as there are conventional T Tauri stars, with the observed spectral energy distributions of the former being quite different from those considered in the present paper (or by KH). The absence of these obscured sources (see the discussion below) makes it unlikely that thick disks are present in many T Tauri systems. Stocke et al. (1987)

---

[1] This result can be easily understood by considering the following simplifications. First, we take the epicyclic frequency to be the circular frequency given by its Keplerian value: $\Omega = \Omega_*(R_*/\varpi)^{3/2}$, where $\Omega_* = (GM_*/R_*^3)^{1/2}$. If the disk temperature is approximated by the power law, $T_D = T_{D*}(R_*/\varpi)^{1/2}$, then $v_T = v_{T*}(R_*/\varpi)^{1/4}$, and equation (17) can be evaluated to get $M_Q \approx 8(H_*/R_*)(R_D/R_*)^{1/4} M_*$, where $H_* = v_{T*}/\Omega_*$ is the scale height at the inner edge of the disk. For typical cases, $H_*/R_* \sim 10^{-2}$ and $R_D/R_* \sim 10^4$, so that $M_Q \sim M_*$.

have suggested that IRS 5 L1551 might be one example, but this object is a famous bipolar flow source with an energy distribution that can be reasonably well fitted by a protostellar model involving infall (in the equatorial directions not affected by the outflow; see Paper I). Bipolar flow sources in general tend to be heavily obscured objects (for a review, see Lada 1985), but selection biases work in favor of detecting such objects *pole-on* rather than equator-on because of the need to disentangle the high-velocity CO from the general emission at the velocity of the ambient molecular cloud. This argues for (rotating) infall as the collimation mechanism rather than static thick disks (see Shu and Terebey 1984). Moreover, T Tauri stars are rarely associated with cold molecular outflows. Thus, bipolar flow sources cannot generally be the edge-on counterparts of optically revealed T Tauri stars, but must represent an earlier phase of young star evolution (Paper I).

What, then, is the true mechanistic explanation for the unorthodox temperature distribution $T_D \propto \varpi^{-1/2}$ *in the disks of flat-spectrum T Tauri stars?* In Paper I, we suggested that the answer might be found in the accretion process of a self-gravitating disk. In this paper, we have shown that although the disks may have large enough masses to make Q of order unity (i.e., the spectrally determined disk masses are not much smaller than $M_\odot$), they almost certainly are not sufficiently massive to introduce significant departures from Keplerian rotation. Since neither viscous accretion in a Keplerian velocity field nor reprocessing of stellar photons in a spatially flat disk can produce the desired effect, we are led to consider the possibility that the mechanism underlying mass and angular momentum transport in the disks of flat-spectrum T Tauri

stars is intrinsically *nonviscous*. In other words, the energy released by accretion may not be dissipated locally, but is transported from the inside to the outside, thereby heating the outer regions of the disk and producing a temperature gradient less steep than the classical result, $T_D \propto \varpi^{-3/4}$. The internal excitation of spiral density waves through nonaxisymmetric gravitational instabilities (see, e.g., the discussion of Lin and Bertin 1985) is one possible mechanism; resonant excitation by a slightly distorted star (e.g., Yuan and Cassen 1985) is another. In any case, collective effects may provide the necessary nonlocal transport indicated by the flat spectral energy distributions of the more extreme T Tauri stars; we believe such waves to contain the promise of the future in the physics of active disks.

APPENDIX

HEATING AND SHADOWING

In this Appendix, we describe the mutual heating and shadowing of a star/disk system. The disk is assumed to be both spatially thin and optically thick (the effects are larger if the disk flares outward or is warped); the star is taken to be spherical. In the Appendix of a previous paper (Adams and Shu 1986), we presented the heating and shadowing formalism for the special case of a classical Keplerian accretion disk. In such a disk, both the intrinsic luminosity and the reprocessed energy from the star produce a temperature distribution that is well represented by the form $T_D \sim \varpi^{-3/4}$, so it suffices to conserve energy "globally," i.e., calculate the total amount of intrinsic and reprocessed luminosity and distribute the energy according to a $T_D \sim \varpi^{-3/4}$ law. However, in the general case considered here, the intrinsic luminosity can produce a temperature distribution quite different from that of the reprocessed stellar energy. Since each element of disk area dA_D must radiate both its intrinsic luminosity and the reprocessed energy, the resulting temperature distribution (corresponding to "local" conservation of energy) cannot be represented as a single power law. The calculation can still be done semianalytically, but the results are more complicated as shown below.

I. HEATING

Consider the mutual heating and shadowing of two elements of area, dA_* with unit normal $\hat{r}$ on the surface of the star and dA_D with unit normal $\hat{z}$ on the surface of the disk. For purposes of integration over the star when dA_D is held fixed, let the vector position of dA_* expressed in spherical polar coordinates be $r_* = (R_*, \theta, \phi)$; of dA_D, $r_D = (\varpi, \pi/2, 0)$. (We assume here that the disk is perfectly thin and flat—see above.) For integration over the disk when dA_* is held fixed, it is preferable to ascribe the azimuthal coordinate ϕ to the disk. A light ray from r_* to r_D has the path vector

$$s\boldsymbol{n} = \boldsymbol{r}_D - \boldsymbol{r}_* , \tag{A1}$$

where s is the path length,

$$s = (R_*^2 + \varpi^2 - 2R_* \varpi \sin \theta \cos \phi)^{1/2} , \tag{A2}$$

and $\boldsymbol{n}$ is the unit propagation vector with the direction cosines:

$$\boldsymbol{n} \cdot \hat{\boldsymbol{r}} = \frac{1}{s} (\boldsymbol{r}_D - \boldsymbol{r}_*) \cdot \hat{\boldsymbol{r}} = \frac{1}{s} (\varpi \sin \theta \cos \phi - R_*) , \tag{A3a}$$

$$\boldsymbol{n} \cdot \hat{\boldsymbol{z}} = \frac{1}{s} (\boldsymbol{r}_D - \boldsymbol{r}_*) \cdot \hat{\boldsymbol{z}} = -\frac{R_*}{s} \cos \theta . \tag{A3b}$$

Here, we assume that there is no appreciable absorption along lines of sight from the star to the disk, so that the rate $d\dot{E}_\nu^*$ at which radiant energy of frequency ν travelling from dA_* is intercepted by dA_D is given by

$$d\dot{E}_\nu^* = I_\nu^*(\mathbf{n} \cdot \hat{r})dA_*(-\mathbf{n} \cdot \hat{z})dA_D/s^2 . \tag{A4}$$

We assume that I_ν^* can be approximated as a Planck function $B_\nu[T(\theta)]$. Integrated over all frequencies and the part of the surface area of the star which can be seen by dA_D, the upper face of the disk at ϖ intercepts, per unit area and time, the amount of energy:

$$\frac{d\dot{E}_*}{dA_D} = \frac{1}{\pi} \int_{\theta_\varpi}^{\pi/2} \sigma T_*^4(\theta) \sin\theta \cos\theta \, d\theta \int_{-\phi_\varpi}^{+\phi_\varpi} \left(\frac{R_*}{s}\right)^4 \left(\frac{\varpi}{R_*} \sin\theta \cos\phi - 1\right) d\phi . \tag{A5}$$

For given θ, the range of the ϕ integration is confined to angles between those where $\mathbf{n} \cdot \hat{r} = 0$, i.e., from $-\phi_\varpi$ to $+\phi_\varpi$, where

$$\cos\phi_\varpi \equiv R_*/\varpi \sin\theta . \tag{A6a}$$

The contribution closest to the pole of the star originates at $\theta = \theta_\varpi$, with

$$\sin\theta_\varpi \equiv R_*/\varpi , \tag{A6b}$$

so that $\phi_\varpi = 0$ at this point.

Here, we assume that the *intrinsic* disk luminosity produces a power-law temperature profile of the form $T_D(\varpi) = T_{D*}(\varpi/R_*)^{-q}$, where $\frac{1}{2} \leq q \leq \frac{3}{4}$. If the disk had only the intrinsic luminosity L_D, integration of the flux over the surface of the disk would imply

$$L_D = 4\pi R_*^2 \sigma T_{D*}^4 \mathscr{D} , \tag{A7a}$$

where the factor $\mathscr{D}$ is defined by

$$\mathscr{D} \equiv \begin{cases} [1 - (R_*/R_D)^{4q-2}]/(4q - 2) , & \text{for } q > \frac{1}{2} ; \\ \ln(R_D/R_*) , & \text{for } q = \frac{1}{2} . \end{cases} \tag{A7b}$$

However, in a steady state the surface of the disk must radiate not only its own accretion energy, but also the intercepted stellar radiation

$$\sigma T_D^4(\varpi) = \left(\frac{L_D}{4\pi R_*^2 \mathscr{D}}\right)\left(\frac{\varpi}{R_*}\right)^{-4q} + \frac{d\dot{E}_*}{dA_D} . \tag{A8}$$

In a similar fashion, the star must radiate not only its intrinsic energy, but also the intercepted disk radiation

$$\sigma T_*^4(\theta) = \frac{L_*}{4\pi R_*^2} + \frac{d\dot{E}_D}{dA_*} , \tag{A9}$$

where L_* is the intrinsic stellar luminosity and where we have assumed a spherically symmetric stellar temperature distribution. In equation (A9), the rate of intercepted disk energy is

$$\frac{d\dot{E}_D}{dA_*} = \frac{1}{\pi} \cos\theta \int_{\varpi_*}^{R_D} \sigma T_D^4(\varpi) \frac{\varpi \, d\varpi}{R_*^2} \int_{-\phi_\varpi}^{+\phi_\varpi} \left(\frac{R_*}{s}\right)^4 \left(\frac{\varpi}{R_*} \sin\theta \cos\phi - 1\right) d\phi , \tag{A10}$$

where

$$\varpi_* \equiv R_*/\sin\theta \tag{A11}$$

is the smallest radius of the disk observable at θ on the star.

Equations (A8) and (A9), together with the subsidiary definitions (A5) and (A10), constitute two coupled integral equations which determine $T_*(\theta)$. Here, we assume $T_*(\theta) = \text{constant} \equiv T_*$. Since it is straightforward to evaluate the reprocessed stellar energy $d\dot{E}_*/dA_D$ in terms of the effective stellar temperature T_* (see eq. [A22] below), the disk temperature profile is completely determined through equations (A5) and (A8). Thus, we need to determine the value T_* so that equations (A8) and (A9) are valid when integrated over the *entire* surfaces of disk and star. It is convenient to first define the effective luminosities by

$$\mathscr{L}_D \equiv \int_{R_*}^{R_D} \sigma T_{D*}^4(\varpi)4\pi\varpi \, d\varpi = L_D + \dot{E}_* , \tag{A12}$$

$$\mathscr{L}_* \equiv 4\pi R_*^2 \sigma T_*^4 = L_* + \dot{E}_D . \tag{A13}$$

Here, $\dot{E}_*$ is the total stellar energy per unit time reprocessed in the disk,

$$\dot{E}_* = 8R_*^2 \sigma T_*^4 \int_{R_*}^{R_D} \frac{\varpi \, d\varpi}{R_*^2} \int_{\theta_\varpi}^{\pi/2} \sin\theta \cos\theta \, d\theta \int_0^{\phi_\varpi} \left(\frac{R_*}{s}\right)^4 \left(\frac{\varpi}{R_*} \sin\theta \cos\phi - 1\right) d\phi , \tag{A14a}$$

and $\dot{E}_D$ is the total disk energy per unit time reprocessed by the star,

$$\dot{E}_D = 8R_*^2 \int_{\theta_{*D}}^{\pi/2} \sin\theta \cos\theta \, d\theta \int_{\varpi_*}^{R_D} \sigma T_D^4(\varpi) \frac{\varpi \, d\varpi}{R_*^2} \int_0^{\phi_\varpi} \left(\frac{R_*}{s}\right)^4 \left(\frac{\varpi}{R_*} \sin\theta \cos\phi - 1\right) d\phi , \tag{A14b}$$

with

$$\sin \theta_{*D} \equiv R_*/R_D \, . \tag{A15}$$

We can write equation (A14a) in the suggestive form

$$\dot{E}_* = f_D \mathscr{L}_* \, , \tag{A16a}$$

which simply states that a fraction f_D of the effective luminosity of the star is intercepted by the disk. For the complementary case of the disk heating the star, the situation is complicated by the fact that the temperature distribution of the disk is composed of two components as expressed in equation (A8). Hence, we can write

$$\dot{E}_D = f_* L_D + f_R \mathscr{L}_* \, , \tag{A16b}$$

where $f_* L_D$ and $f_R \mathscr{L}_*$ are the amounts of the intrinsic disk luminosity and the reprocessed luminosity (respectively) intercepted by the star.

If we now introduce a transformation of variables,

$$u \equiv R_*/\varpi \, , \qquad v \equiv \sin \theta \, , \qquad w \equiv \cos \phi \, , \tag{A17}$$

and switch one order of integration, we can express f_D, f_*, and f_R as the dimensionless integrals

$$f_D = \frac{2}{\pi} \int_{u_{*D}}^{1} h(u)du \, , \qquad f_* = \frac{2}{\pi \mathscr{D}} \int_{u_{*D}}^{1} u^{4q} h(u)du \, , \tag{A18a}$$

$$f_R = \frac{2}{\pi^2} \int_{u_{*D}}^{1} [\arcsin u - u(1 - u^2)^{1/2}] h(u)du \, , \tag{A18b}$$

$$h(u) \equiv \int_{u}^{1} v \, dv \int_{u/v}^{1} \frac{(vw - u)dw}{(1 - w^2)^{1/2}(1 + u^2 - 2uvw)^2} \, , \tag{A18c}$$

with $u_{*D} \equiv R_*/R_D$. By a judicious change of variables (motivated by switching to a spherical coordinate system where the line joining the center of the star and the disk point is the polar axis), we can integrate equation (A18c) to get

$$h(u) = \frac{1}{2u^3} [\arcsin u - u(1 - u^2)^{1/2}] \, . \tag{A18d}$$

Notice that we have used the result (A18d) in writing the expression (A18b) for f_R.

The analytic form of the function $h(u)$, as given by equation (A18d), allows us to evaluate f_D through the expression (A18a), which now yields

$$f_D = \frac{1}{4} - \frac{1}{\pi} \left[\left(1 - \frac{1}{2u_{*D}^2} \right) \arcsin u_{*D} + \frac{1}{2u_{*D}} (1 - u_{*D}^2)^{1/2} \right] \, . \tag{A19}$$

The integral for f_* can be solved only in the special case where $4q$ is an integer; in general, for $\frac{3}{4} > q > \frac{1}{2}$, the function f_* can be expressed

$$f_* = \frac{1}{(4q - 2)\mathscr{D}\pi} \left\{ \frac{\pi}{2} - u_{*D}^{4q-2} [\arcsin u_{*D} - u_{*D}(1 - u_{*D}^2)^{1/2}] - 2 \int_{u_{*D}}^{1} u^{4q}(1 - u^2)^{-1/2} \, du \right\} \, . \tag{A20a}$$

For the special case $q = \frac{1}{2}$, the function f_* takes the form

$$f_* = \frac{1}{2\mathscr{D}\pi} \left[u_{*D}(1 - u_{*D}^2)^{1/2} + (1 - 2 \ln u_{*D}) \arcsin u_{*D} - \frac{\pi}{2} - 2 \int_{u_{*D}}^{1} \ln u (1 - u^2)^{-1/2} \, du \right] \, , \tag{A20b}$$

whereas for the case $q = \frac{3}{4}$,

$$f_* = \frac{1}{\mathscr{D}\pi} \left[\frac{\pi}{2} - u_{*D} \arcsin u_{*D} - \frac{1}{3} (1 - u_{*D}^2)^{1/2}(4 - u_{*D}^2) \right] \, . \tag{A20c}$$

The function f_R is independent of the temperature index q and can be easily evaluated:

$$f_R = \left(\frac{1}{8} - \frac{1}{\pi^2} \right) + \frac{1}{\pi^2} \left\{ \frac{1}{2u_{*D}^2} [\arcsin u_{*D} - u_{*D}(1 - u_{*D}^2)^{1/2}]^2 + (\arcsin u_{*D})^2 - u_{*D}^2 \right\} \, . \tag{A21}$$

The result (A18d), along with equations (A5) and (A8), allows us to write the disk temperature distribution as

$$\sigma T_D^4(\varpi) = \left[\frac{L_D}{4\pi R_*^2 \mathscr{D}} \right] \left(\frac{\varpi}{R_*} \right)^{-4q} + \frac{1}{\pi} \sigma T_*^4 [\arcsin u - u(1 - u^2)^{1/2}] \, , \tag{A22}$$

where the second term is the reprocessed stellar luminosity $d\dot{E}_*/dA_D$. Thus, the temperature distribution of both the star and the disk are determined once T_* is specified.

With f_* and f_R specified as shown above, equations (A13) and (A16) can be combined to determine the effective stellar luminosity (or equivalently the effective stellar temperature):

$$\mathscr{L}_* = 4\pi R_*^2 \sigma T_*^4 = \frac{1}{1 - f_R}(L_* + f_* L_D) \,. \tag{A23}$$

Notice that heating of the star and disk through the interception of each other's photons makes both objects hotter than the naive predictions with no interaction,

$$\sigma T_*^4 = \frac{L_*}{4\pi R_*^2} \qquad \text{and} \qquad \sigma T_D^4(\varpi) = \frac{L_D}{4\pi R_*^2 \mathscr{D}}\left(\frac{\varpi}{R_*}\right)^{-4q} \,.$$

This effect is especially important for the disk whenever L_* is comparable to or larger than L_D. Mutual warming occurs because the star and disk have to radiate their respective luminosities, L_* and L_D, through the *same* 4π steradians of sky, whereas the above equations assume that both the star and disk each have their individual 4π steradians. The entire sky, of course, always receives only $L = L_* + L_D$ since mutual eclipses of star and disk *automatically* cancel the increased radiation from clear lines of sight, provided that heating and shadowing are done self-consistently. (The energy of every stellar photon absorbed and reradiated by the disk is not available to travel in its original state to some distant observer. In the theory of the light curves of binary stars, the effect is known as "reflection.") To see this explicitly in the present context, we proceed now to consider the effects of shadowing.

II. SHADOWING

In the plane of the sky, construct (x, y) coordinates with origin centered on the star and with the y-axis aligned along the projected rotation axis. The locus of the outer edge of the disk satisfies the equation

$$\frac{x^2}{R_D^2} + \frac{y^2}{R_D^2 \cos^2 \theta} = 1 \,, \tag{A24a}$$

that of the limb of the star satisfies

$$x^2 + y^2 = R_*^2 \,, \tag{A24b}$$

and that of the inner edge of the disk satisfies

$$\frac{x^2}{R_*^2} + \frac{y^2}{R_*^2 \cos^2 \theta} = 1 \,. \tag{A24c}$$

Since we have assumed the face of the star to be uniformly bright, the geometrical factor g_D by which disk blocking reduces the naive expression for the stellar flux equals $1 - A_*/\pi R_*^2$, where A_* is the projected area of the part of the star behind the disk.

When $\cos \theta \geq u_{*D}$, the outer edge of the disk lies beyond the limb of the star everywhere and g_D is easily computed as

$$g_D = \frac{1}{2}(1 + \cos \theta) \,. \tag{A25}$$

When $\cos \theta \leq u_{*D}$, let (x_*, y_*) be the coordinates of the intersection of curves (A24a) and (A24b), i.e.,

$$x_* = R_* \xi_* \,, \qquad \text{where } \xi_* \equiv \frac{(1 - \cos^2 \theta/u_{*D}^2)^{1/2}}{\sin \theta} \tag{A26}$$

is less than 1 for $u_{*D} \leq 1$. With these definitions, A_* is easily computed as

$$A_* = 2\left(\int_0^{x_*} dx \int_{y_c(x)}^{y_a(x)} dy + \int_{x_*}^{R_*} dx \int_{y_c(x)}^{y_b(x)} dy\right) \,, \tag{A27}$$

where $y_a(x)$, $y_b(x)$, and $y_c(x)$ are, respectively, the positive solutions of y as functions of x obtained, respectively, from equations (A24a), (A24b), and (A24c). We can now introduce the variable transformation, $x \equiv R_* \xi$, and integrate equation (A27) to obtain A_* and therefore g_D:

$$g_D = \frac{1}{2}(1 + \cos \theta) + \frac{1}{\pi}\left[\arcsin \xi_* - \frac{\cos \theta}{u_{*D}^2} \arcsin (u_{*D} \xi_*)\right] \,, \tag{A28}$$

where we have made use of the identity

$$\xi_*\left[(1 - \xi_*^2)^{1/2} - \frac{\cos \theta}{u_{*D}}(1 - u_{*D}^2 \xi_*^2)^{1/2}\right] = 0 \,.$$

Notice that formulae (A25) and (A28) are in agreement for $\cos \theta = u_{*D}$, i.e., for $\xi_* = 0$.

An area A_D of the disk is shadowed by the star which is numerically equal to A_*. When $\cos \theta \leq u_{*D}$, the radiant flux is not reaching a distant observer is

$$\Delta F_D = \frac{2}{\pi r^2} \left[\int_0^{x_*} dx \int_{y_c(x)}^{y_a(x)} \sigma T_D^4(\varpi) dy + \int_{x_*}^{R_*} dx \int_{y_c(x)}^{y_b(x)} \sigma T_D^4(\varpi) dy \right], \tag{A29}$$

where

$$\varpi^2 = x^2 + \frac{y^2}{\cos^2 \theta}$$

and $\sigma T_D^4(\varpi)$ is given by equation (A22). (Notice that when $\cos \theta \geq u_{*D}$, $x_* = 0$ and the first term in eq. [A29] above vanishes.)

Again, since the disk temperature distribution contains two components (the first from the intrinsic luminosity, the second from reprocessing), it is convenient to decompose ΔF_D into two parts. If we first introduce the successive transformations, $x \equiv R_* \xi$, $y \equiv R_* \eta \cos \theta$, and $\xi \equiv v \cos \phi$, $\eta \equiv v \sin \phi$, and finally $u \equiv 1/v$, the expression (A29) for ΔF_D can be written

$$\Delta F_D = 2 \cos \theta \left(\frac{R_*}{r}\right)^2 \left(\frac{L_D}{4\pi R_*^2 \mathscr{D}} \mathscr{G}_* + \sigma T_*^4 \mathscr{H}_*\right), \tag{A30}$$

where $\mathscr{G}_*$ and $\mathscr{H}_*$ are given by

$$\mathscr{G}_* \equiv \frac{1}{\pi} \left[\int_{\phi_*}^{\pi/2} d\phi \int_{u_{*D}}^1 u^{4q-3} du + \int_0^{\phi_*} d\phi \int_{(\cos^2 \phi + \cos^2 \theta \sin^2 \phi)^{1/2}}^1 u^{4q-3} du \right], \tag{A31a}$$

$$\mathscr{H}_* \equiv \frac{2}{\pi^2} \left[\int_{\phi_*}^{\pi/2} d\phi \int_{u_{*D}}^1 h(u) du + \int_0^{\phi_*} d\phi \int_{(\cos^2 \phi + \cos^2 \theta \sin^2 \phi)^{1/2}}^1 h(u) du \right], \tag{A31b}$$

with ϕ_* defined by

$$\phi_* \equiv \begin{cases} \arccos(u_{*D} \xi_*), & \text{for } \cos \theta \leq u_{*D}, \\ \pi/2, & \text{for } \cos \theta \geq u_{*D}. \end{cases} \tag{A32}$$

For $q > \frac{1}{2}$, equation (A31a) can be simplified to the form

$$\mathscr{G}_* = \frac{1}{2} \mathscr{D} + \frac{1}{\pi(4q-2)} \left[u_{D*}^{4q-2} \phi_* - \int_0^{\phi_*} (\cos^2 \phi + \cos^2 \theta \sin^2 \phi)^{2q-1} d\phi \right], \tag{A33a}$$

whereas, for the case $q = \frac{1}{2}$, $\mathscr{G}_*$ takes the form

$$\mathscr{G}_* = \frac{1}{\pi} \mathscr{D} \left(\frac{\pi}{2} - \phi_*\right) - \frac{1}{2\pi} \int_0^{\phi_*} \ln(\cos^2 \phi + \cos^2 \theta \sin^2 \phi) d\phi. \tag{A33b}$$

It is also convenient to consider separately the special case $q = \frac{3}{4}$, which is the expected result for a classical Keplerian accretion disk; then $\mathscr{G}_*$ becomes

$$\mathscr{G}_* = \frac{1}{2} \mathscr{D} + \frac{1}{\pi} [u_{D*} \phi_* - E(\sin \theta, \phi_*)], \tag{A33c}$$

where $E(\sin \theta, \phi_*)$ is the incomplete elliptic integral of the second kind,

$$E(\sin \theta, \phi_*) \equiv \int_0^{\phi_*} (1 - \sin^2 \theta \sin^2 \phi)^{1/2} d\phi.$$

Notice that for $\cos \theta \geq u_{D*}$, $\phi_* = \pi/2$, and the above integral becomes the complete elliptic integral of the second kind.

The expression (A31b) for $\mathscr{H}_*$ simplifies to

$$\mathscr{H}_* = \frac{1}{\pi} \left(\frac{\pi}{2} - \phi_*\right) f_D + \frac{1}{4\pi} \phi_* - \frac{1}{2\pi^2} \int_0^{\phi_*} d\phi \left[Z^{-1/2} \sin \phi \sin \theta + \left(2 - \frac{1}{Z}\right) \arcsin Z^{1/2} \right], \tag{A34}$$

where

$$Z \equiv \cos^2 \phi + \cos^2 \theta \sin^2 \phi.$$

Since the naked disk flux F_N can be written

$$F_N = \frac{2 \cos \theta}{4\pi r^2} \mathscr{L}_D = \frac{2 \cos \theta}{4\pi r^2} (L_D + f_D L_*), \tag{A35}$$

the geometrical factor for stellar shadowing of the disk becomes

$$g_* = 1 - \frac{L_D}{\mathscr{D} \mathscr{L}_D} \mathscr{G}_* - \frac{\mathscr{L}_*}{\mathscr{L}_D} \mathscr{H}_*. \tag{A36}$$

III. CONSERVATION OF LUMINOSITY

The (unattenuated) luminosity of the central source at radius r is

$$L_c = \int_0^{\pi/2} 4\pi r^2 [F_*^{(0)} + F_D^{(0)}] \sin \theta \, d\theta \,, \tag{A37}$$

where

$$4\pi r^2 F_*^{(0)} = \mathscr{L}_* g_D \quad \text{and} \quad 4\pi r^2 F_D^{(0)} = \mathscr{L}_D 2g_* \cos \theta \,. \tag{A38}$$

Here, g_D and g_* are given as functions of θ by equations (A25) and (A36) when $\cos \theta \geq u_{*D}$ and by equations (A28) and (A36) when $\cos \theta \leq u_{*D}$; T_* is determined through equation (A23). If we have self-consistently accounted for heating and shadowing, L_c should equal $L_* + L_D$. This assertion can be easily verified by noting that the heating and shadowing factors calculated above satisfy the identities

$$G_D \equiv \int_0^{\pi/2} g_D \sin \theta \, d\theta = 1 - f_D \,, \tag{A39a}$$

$$G_* \equiv \int_0^{\pi/2} 2g_* \cos \theta \sin \theta \, d\theta = 1 - \frac{L_D}{\mathscr{L}_D} f_* - \frac{\mathscr{L}_*}{\mathscr{L}_D} f_R \,. \tag{A39b}$$

Hence,

$$L_c = \mathscr{L}_*(1 - f_D) + \mathscr{L}_D - (f_* L_D + f_R \mathscr{L}_*) \,, \tag{A40}$$

which can be combined with equations (A12), (A13), and (A16) to show that $L_c = L_* + L_D$.

It is easy to understand the physical interpretation of equations (A39). The quantity $\mathscr{L}_*$ is the "effective" luminosity of the star—the luminosity that would be observed in the absence of shadowing by the disk (but including heating of the star by the disk). Since $G_D \mathscr{L}_*$ is the actual observed (unattenuated) luminosity from the star and $f_D \mathscr{L}_*$ is the stellar luminosity reprocessed in the disk, it follows that $G_D \mathscr{L}_* + f_D \mathscr{L}_* = \mathscr{L}_*$. Similarly, $\mathscr{L}_D$ is the "effective" luminosity of the disk. Then $G_* \mathscr{L}_D$ is the observed luminosity from the disk, which is equal to the effective luminosity $\mathscr{L}_D$ *minus* the quantity $(f_* L_D + f_R \mathscr{L}_*)$, which is the sum of the intrinsic and reprocessed components of the disk luminosity intercepted by the star. Thus, equations (A39) simply express conservation of energy.

IV. LIMITING FORMS

Since $R_D \gg R_*$ for most cases of interest, it is convenient to use the $u_{*D} \to 0$ limiting forms of the heating and the shadowing factors. In this limit,

$$f_D = \frac{1}{4} \,, \qquad f_R = \frac{1}{8} - \frac{1}{\pi^2} \,, \qquad \text{and} \quad g_D = \frac{1}{2}(1 + \cos \theta) \,. \tag{A41}$$

However, the corresponding expressions for f_* and g_* depend on the temperature profile index q and are more complicated. For the case $q > \frac{1}{2}$, these factors can be expressed as

$$f_* = \frac{1}{2} - \frac{2}{\pi} \int_0^1 u^{4q}(1 - u^2)^{-1/2} \, du \tag{A42a}$$

and

$$g_* = 1 + \frac{L_D}{\mathscr{L}_D} \left[\frac{1}{\pi} \int_0^{\pi/2} (\cos^2 \phi + \cos^2 \theta \sin^2 \phi)^{2q-1} \, d\phi - \frac{1}{2} \right] - \frac{\mathscr{L}_*}{\mathscr{L}_D} \mathscr{H}_0 \,, \tag{A42b}$$

where $\mathscr{H}_0$ is the limiting form of equation (A34), which can be expressed as

$$\mathscr{H}_0 = \frac{1}{8} - \frac{1}{2\pi^2} \int_0^{\pi/2} d\phi \left[Z^{-1/2} \sin \phi \sin \theta + \left(2 - \frac{1}{Z}\right) \arcsin Z^{1/2} \right] \,,$$

with $Z = \cos^2 \phi + \cos^2 \theta \sin^2 \phi$ as before.

For the special case $q = \frac{3}{4}$, the heating and shadowing factors have relatively simple forms,

$$f_* = \frac{1}{2} - \frac{4}{3\pi} \tag{A43a}$$

and

$$g_* = 1 + \frac{L_D}{\mathscr{L}_D} \left[\frac{1}{\pi} E(\sin \theta, \pi/2) - \frac{1}{2} \right] - \frac{\mathscr{L}_*}{\mathscr{L}_D} \mathscr{H}_0 \,, \tag{A43b}$$

where $E(\sin \theta, \pi/2)$ is the complete elliptic integral of the second kind. For the other special case of interest, $q = \frac{1}{2}$, taking the $u_{*D} \to 0$ limit is complicated by the fact that the luminosity of the disk is logarithmically divergent. If we keep terms to order $[\ln (1/u_{*D})]^{-1}$ (i.e. to order $\mathcal{D}^{-1}$),

$$f_* = \frac{1}{2\mathcal{D}} \left(\ln 2 - \frac{1}{2} \right) \tag{A44a}$$

and

$$g_* = 1 + \frac{L_D}{\mathscr{L}_D} \frac{1}{2\mathcal{D}} \ln \left(\frac{1 + \cos \theta}{2} \right) - \frac{\mathscr{L}_*}{\mathscr{L}_D} \mathscr{H}_0 . \tag{A44b}$$

Notice that in the formal limit $u_{*D} \to 0$, the quantity $\mathcal{D} \to \infty$ so that $f_* \to 0$ and $g_* \to 1 - \mathscr{H}_0 \mathscr{L}_*/\mathscr{L}_D$. The physical interpretation of $f_* \to 0$ is that the fraction of the intrinsic disk luminosity (which is logarithmically divergent) that is reprocessed by the star becomes zero. The limiting form of the shadowing factor expresses the fact that all of the intrinsic disk luminosity can be seen by an observer at infinity, whereas a given fraction of the reprocessed luminosity is intercepted by the star.

V. ANGULAR DEPENDENCE OF INFERRED LUMINOSITY

One important consequence of the heating and shadowing effects discussed in this Appendix is the relation between the "observed" luminosity,

$$L_{\mathrm{obs}} \equiv 4\pi r^2 \int F_\nu^{\mathrm{obs}} d\nu ,$$

and the true intrinsic luminosity, $L = L_* + L_D$, of the system. For a given viewing angle θ and no attenuation, it is straightforward to express the "observed" stellar and disk fluxes L_*^{obs} and L_D^{obs} (obtained by integrating eqs. [7] and [9] over all frequencies) in terms of the intrinsic luminosities L_* and L_D and the heating and shadowing functions derived above:

$$L_D^{\mathrm{obs}}(\theta) = 2g_*(\theta) \cos \theta \left[L_D + \frac{f_D}{1 - f_R} (L_* + f_* L_D) \right] , \tag{A45a}$$

$$L_*^{\mathrm{obs}}(\theta) = g_D(\theta) \frac{1}{1 - f_R} (L_* + f_* L_D) . \tag{A45b}$$

REFERENCES

Adams, F. C., Lada, C. J., and Shu, F. H. 1987, *Ap. J.*, **213**, 788 (Paper I).
Adams, F. C., and Shu, F. H. 1985, *Ap. J.*, **296**, 655.
———. 1986, *Ap. J.*, **308**, 836.
Alexander, D. R., Johnson, H. R., and Rypma, R. L. 1983, *Ap. J.*, **272**, 773.
Allamandola, L. J., Tielens, A. G. G. M., and Barker, J. R. 1985, *Ap. J. (Letters)*, **290**, L25.
Beall, J. H. 1987, *Ap. J.*, **316**, 227.
Beckwith, S., Sargent, A. I., Scoville, N. Z., Masson, C. R., Zuckerman, B., and Phillips, T. G. 1986, *Ap. J.*, **309**, 755.
Beckwith, S., Zuckerman, B., Skrutskie, M. F., and Dyck, H. M. 1984, *Ap. J.*, **287**, 793.
Bertout, C. 1987, in *IAU Symposium 122, Circumstellar Matter*, ed. J. Appenzeller and C. Jordan (Dordrecht: Reidel), p. 23.
Bertout, C., Basri, G., and Bouvier, J. 1987, *Ap. J.*, submitted.
Borderies, N., Goldreich, P., and Tremaine, S. 1985, *Icarus*, **63**, 406.
Cohen, M. 1973, *M.N.R.A.S.*, **161**, 97.
———. 1975, *M.N.R.A.S.*, **173**, 279.
———. 1980, *M.N.R.A.S.*, **191**, 499.
———. 1983, *Ap. J. (Letters)*, **270**, L69.
———. 1984, *Phys. Rept.*, Vol. **116**, No. 4, p. 173.
Cohen, M., and Kuhi, L. V. 1979, *Ap. J. Suppl.*, **41**, 743.
Cohen, M., and Schwartz, R. D. 1976, *M.N.R.A.S.*, **174**, 137.
Cohen, M., Tielens, A. G. G. M., and Allamandola, L. J. 1985, *Ap. J. (Letters)*, **299**, L93.
Draine, B. T., and Lee, H. M. 1984, *Ap. J.*, **285**, 89.
Dyck, H. M., Simon, T., and Zuckerman, B. 1982, *Ap. J. (Letters)*, **255**, L103.
Edwards, S., Cabrit, S., Strom, S. E., Heyer, I., Strom, K. M., and Anderson, E. 1987, *Ap. J.*, in press.
Elias, J. H. 1978, *Ap. J.*, **224**, 857.
Elmegreen, B. G. 1982a, *Ap. J.*, **253**, 655.
———. 1982b, in *Formation of Planetary Systems*, ed. A. Brahic (Toulouse: Cepadues Editions), p. 63.
Friedjung, M. 1985, *Astr. Ap.*, **146**, 366.
Grasdalen, G. L., Strom, K. M., Capps, R. W., Thompson, D., and Castelaz, M. 1984, *Ap. J. (Letters)*, **283**, L57.
Hanson, R. B., Jones, B. F., and Lin, D. N. C. 1983, *Ap. J. (Letters)*, **270**, L27.
Hartmann, L., and Kenyon, S. J. 1985, *Ap. J.*, **299**, 462.
———. 1987, *Ap. J.*, **312**, 243.

Hayashi, C., Hoshi, R., and Sugimoto, D. 1962, *Prog. Theor. Phys. Suppl.*, No. 22.
Herbig, G. H., and Rao, K. 1972, *Ap. J.*, **174**, 401.
Hildebrand, R. H. 1983, *Quart. J.R.A.S.*, **24**, 267.
Hunter, C., and Toomre, A. 1969, *Ap. J.*, **155**, 747.
Iben, I. 1965, *Ap. J.*, **141**, 993.
Keyon, S. J., and Hartmann, L. 1987, *Ap. J.*, in press.
Lada, C. J. 1985, *Ann. Rev. Astr. Ap.*, **23**, 267.
———. 1987, in *IAU Symposium 115 Star Forming Regions*, ed. M Peimbert and J. Jugaku (Dordrecht: Reidel), in press.
Lada, C. J., and Wilking, B. A. 1984, *Ap. J.*, **287**, 610.
Leger, A., and Puget, J. L. 1984, *Astr. Ap.*, **137**, L5.
Lin, C. C., and Bertin, G. 1985, in *IAU Symposium 106, The Milky Way*, ed. H. van Woerden, R. J. Allen, and W. B. Burton (Dordrecht: Reidel), p. 513.
Lin, D. N. C., and Papaloizou, J. 1979, *M.N.R.A.S.*, **186**, 799.
———. in *Protostars and Planets II*, ed. D. C. Black and M. S. Matthews (Tucson: University of Arizona Press), p. 981.
Lin, D. N. C., and Pringle, J. E. 1987, preprint.
Lynden-Bell, D., and Pringle, J. E. 1974, *M.N.R.A.S.*, **168**, 603.
Mendoza, E. E. V. 1966, *Ap. J.*, **143**, 1010.
———. 1968, *Ap. J.*, **151**, 977.
Mercer-Smith, J. A., Cameron, A. G. W., and Epstein, R. I. 1984, *Ap. J.*, **279**, 363.
Parker, E. N. 1966, *Ap. J.*, **145**, 811.
Paczynski, B. 1978, *Acta Astr.*, **28**, 91.
Quirk, W. J. 1972, *Ap. J. (Letters)*, **176**, L9.
Rowan-Robinson, M., and Harris, S. 1982, *M.N.R.A.S.*, **200**, 197.
Rowan-Robinson, M., Lock, T. D., Walker, W., and Harris, S. 1986, *M.N.R.A.S.*, **222**, 273.
Rucinski, S. M. 1985, *A. J.*, **90**, 2321.
Rydgren, A. E., Schmelz, J. T., and Vrba, F. J. 1982, *Ap. J.*, **256**, 168.
Rydgren, A. E., Schmelz, J. T., Zak, D. S., and Vrba, F. J. 1984, *Broad Band Spectral Energy Distributions of T Tauri Stars in the Taurus-Auriga Region*, Pub. US Naval Obs., 2d Ser. Vol. **25**, p. 1.
Rydgren, A. E., Strom, S. E., and Strom, K. M. 1976, *Ap. J. Suppl.*, **30**, 307.
Rydgren, A. E., and Vrba, F. J. 1981, *A.J.*, **86**, 725.
———. 1983, *A.J.*, **88**, 1017.
Rydgren, A. E., and Zak, D. S. 1987, *Pub. A.S.P.*, **99**, 141.

Sargent, A. I., and Beckwith, S. 1987, *Ap. J.*, submitted.
Sellgren, K. 1984, *Ap. J.*, **277**, 623.
Shu, F. H. 1974, *Astr. Ap.*, **33**, 55.
Shu, F. H., Adams, F. C., and Lizano, S. 1987, *Ann. Rev. Astr. Ap.*, **25**, 23.
Shu, F. H., Cuzzi, J. N., and Lissauer, J. J. 1983, *Icarus*, **53**, 185.
Shu, F. H., Dones, L., Lissauer, J. J., Yuan, C., and Cuzzi, J. N. 1985, *Ap. J.*, **299**, 542.
Shu, F. H., and Terebey, S. 1984, in *Cool Stars and Stellar Systems*, ed. S. Baliunas and L. Hartmann (Berlin: Springer-Verlag), p. 78.
Stocke, J., Hartigan, P., Strom, S. E., Strom, K. M., Anderson, E. R., Hartmann, L. W., and Kenyon, S. A. 1987, preprint.
Stringfellow, G. 1987, *Bull. AAS*, **18**, 1028.

Strom, S. E., Strom, K. M., and Vrba, F. J. 1976, *A.J.*, **81**, 320.
Terebey, S., Shu, F. H., and Cassen, P. 1984, *Ap. J.*, **286**, 529.
Toomre, A. 1964, *Ap. J.*, **139**, 1217.
Yaun, C., and Cassen, P. 1985, *Icarus*, **64**, 435.
Walker, C. K., Adams, F. C., and Lada, C. J. 1987, in preparation.
Walter, F. W. 1987, *Pub. A.S.P.*, in press.
Weidenschilling, S. J. 1980, *Icarus*, **44**, 172.
———. 1984, *Icarus*, **60**, 553.
Weintraub, D. A., Masson, C. R., and Zuckerman, B. 1987, *Ap. J.*, **320**, in press.
Wetherill, G. W. 1980, *Ann. Rev. Astr. Ap.*, **18**, 77.
Wolfire, M. G., and Churchwell, E. 1987, *Ap. J.*, in press.

Fred C. Adams: Physics and Astronomy Departments, University of California, Berkeley, CA   94720

Charles J. Lada: Steward Observatory, University of Arizona, Tucson, AZ   85721

Frank H. Shu: Astronomy Department, University of California, Berkeley, CA   94720